

Abundances of disk and bulge giants from hi-res optical spectra[★]

I. O, Mg, Ca, and Ti in the Solar neighborhood and Kepler field samples

H. Jönsson^{1,2,3}, N. Ryde¹, T. Nordlander⁴, A. Pehlivan^{1,5}, H. Hartman^{1,5}, P. Jönsson⁵, and K. Eriksson⁴

¹ Lund Observatory, Department of Astronomy and Theoretical Physics, Lund University, Box 43, SE-221 00 Lund, Sweden
e-mail: henrikj@astro.lu.se

² Instituto de Astrofísica de Canarias (IAC), E-38205 La Laguna, Tenerife, Spain

³ Universidad de La Laguna, Dpto. Astrofísica, E-38206 La Laguna, Tenerife, Spain

⁴ Department of Physics and Astronomy, Uppsala University, Box 516, SE-751 20 Uppsala, Sweden

⁵ Materials Science and Applied Mathematics, Malmö University, SE-205 06 Malmö, Sweden

Submitted 2016; accepted 2016

ABSTRACT

Context. The galactic bulge is an intriguing and significant part of our galaxy, but it is hard to observe, being both distant and covered by dust in the disk. Therefore there do not exist many high-resolution optical spectra of bulge stars with large wavelength coverage, whose determined abundances can be compared with nearby, similarly analyzed stellar samples.

Aims. We aim to determine the, for chemical evolution models, so important alpha elements of a sample of bulge giants using high-resolution optical spectra with large wavelength coverage. The abundances found will be compared to similarly derived abundances from similar spectra of similar stars in the local thin and thick disks. In this first paper we focus on the Solar neighborhood reference sample.

Methods. We use spectral synthesis to derive the stellar parameters as well as the elemental abundances of both the local as well as the bulge samples of giants. Special care is taken to benchmark our method of determining stellar parameters against independent measurements of effective temperatures from angular diameter measurements and surface gravities from asteroseismology.

Results. In this first paper we present the method used to determine the stellar parameters as well as the elemental abundances, evaluate them, and present the results for our local disk sample of 291 giants.

Conclusions. When comparing our determined spectroscopic temperatures to those derived from angular diameter measurements, we reproduce these with a systematic difference of +10 K and a standard deviation of 53 K. The spectroscopic gravities are reproducing the ones determined from asteroseismology with a systematic offset of +0.10 dex and a standard deviation of 0.12 dex. When it comes to the abundance trends, our sample of local disk giants is closely following that of other works analyzing solar neighborhood dwarfs, showing that the much brighter giant stars are as good abundance probes as the often used dwarfs.

Key words. Galaxy: solar neighborhood – Galaxy: evolution – Stars: abundances

1. Introduction

How the galactic bulge formed and evolved is an intriguing question that is been given a lot of attention the last years (see for example Rich 2013; Gonzalez & Gadotti 2015; Di Matteo 2016, for reviews). There are three problems with observing the bulge; it is distant, so the stars are faint, it is obscured by the dust in the disk, so very little of the optical light emitted by the bulge stars reach us, and the crowding of stars is making it hard to place the spectrometer's slit to avoid contaminating light from another star. For the first two problems it helps to observe luminous giant stars, and indeed this has been the main method used, see for example Zoccali et al. (2006); Lecureur et al. (2007); Alves-Brito et al. (2010); González et al. (2011); Johnson et al. (2012, 2013, 2014).

[★] Based on observations made with the Nordic Optical Telescope (programs 51-018 and 53-002), operated by the Nordic Optical Telescope Scientific Association at the Observatorio del Roque de los Muchachos, La Palma, Spain, of the Instituto de Astrofísica de Canarias, and on spectral data retrieved from PolarBase at Observatoire Midi Pyrénées.

One fact that could cause problems when analysing spectra from giant stars, is the presence of molecules in their atmospheres. The molecules emerge since giant stars are generally cooler than the dwarf stars often used in spectroscopic investigations. A complication is therefore the increased number of lines, mainly due to the rich molecular spectra. This might lead, particularly for the very coolest and most metal-rich stars, to the situation where the continuum close to lines of interest can not be identified even at very high spectral resolution. Since the abundance derived from a spectral line depends on the ratio of line to continuum opacities, large uncertainties will be introduced if the continuum can not be defined. A large density of lines might also form a pseudo-continuum, which falsely might be taken as a true continuum, further complicating the analysis. The probability of spectral lines being blended, in the worst case by unknown lines or lines with uncertain line data, is increased by the molecular lines. The spectral lines of choice to use in an abundance analysis, which are as unblended as possible and not too deep, might therefore be rare. As this problem is worse the cooler a star is, many works, including the bulge-articles mentioned in the first paragraph (and this project), have restricted themselves to the moderately cool K-giants or red clump stars.

Furthermore, for sun-like stars, the abundance could be determined differentially by simply comparing the strength of the spectral line in question in the stellar spectrum to that of a solar spectrum. Such an approach for an analysis of giants is more complicated, and might introduce large systematic uncertainties: if a solar spectrum is used in the comparison, in many cases unknown blending lines show up in the giant star spectra, leading to an overestimation of the abundance of the element in the giant star, and if instead a spectrum of a giant star is used as a comparison, the zero-point of the derived abundances are very uncertain, because they rely on the accuracy of the abundances and stellar parameters of the comparison star, as well as the completeness of the linelist.

To deal with these problems when giant stars are used in abundance works investigating for example the bulge, a good approach is to make a strictly differential comparison between the abundances found in the bulge to that of the more known stellar population of the local disk. For example, Alves-Brito et al. (2010), found elemental abundances from their 25 bulge giants to be similar to that of the thick disk in their 55 similar giants from the Solar neighborhood, and Bensby et al. (2013), using microlensed dwarfs, found that the ‘knee’ in their $[\alpha/\text{Fe}]$ vs. $[\text{Fe}/\text{H}]$ -plots likely was at slightly higher metallicities in their 58 bulge dwarfs as compared to their local disk sample of 714 stars (Bensby et al. 2014).

In this paper we present a compilation of a solar neighborhood sample of 291 local disk giants for which we have determined the stellar parameters and the abundances of the α elements oxygen, magnesium, calcium, and titanium. We demonstrate that we can determine the elemental abundances of giants with similar precision and accuracy as for dwarfs. In Paper II of this series, we will use this solar neighborhood sample to differentially compare elemental abundances of giants in the bulge to abundances in the solar neighborhood. This will be possible since we will determine the stellar parameters and α abundances of the bulge sample in the same way.

The homogeneously analyzed local disk sample presented here, might also be useful in other aspects: since it includes stars in the Kepler field, the determined parameters might be used to revise the stellar properties for these stars (Huber et al. 2014), or the bright stars of the sample might be used as a basis for selecting and analyzing stars using smaller telescopes and/or less sensitive instruments, as for example the MIR spectrometer TEXES (Lacy et al. 2002). To our knowledge, the sample presented here is the largest spectroscopically analyzed sample of metal-rich giants using high-resolution optical spectra with large wavelength coverage.

2. Observations

2.1. The bulge sample

As mentioned in Section 1, the main purpose of this project is to analyze high-resolution optical spectra of bulge giants, but the analysis of the actual bulge spectra will be presented in Paper II of the series, while this paper concentrates on the analysis of a local disk comparison sample. The bulge sample consists of 46 K-giants observed with FLAMES/UVES at VLT, and consists of 35 spectra that have been previously analyzed in Zoccali et al. (2006), Lecureur et al. (2007), Ryde et al. (2010), Barbuy et al. (2013), and Van der Swaelmen et al. (2016) as well as 11 never before analyzed spectra from a new bulge field even closer to the galactic center with $(l, b) = (1.25, -2.65)$. More details on this sample will be given in Paper II.

2.2. The Solar neighborhood sample

In this paper, Paper I in the series, we present the analysis of 291 giants in the Solar neighborhood: 150 were observed by us using the spectrometer FIES (Telting et al. 2014) mounted on the Nordic Optical Telescope (NOT) under program 51-018 (May-June 2015), 63 more stars were observed by us using FIES/NOT under program 53-002 (June 2016), 41 spectra were taken from Thygesen et al. (2012) (in turn from FIES/NOT), 18 spectra were downloaded from the FIES-archive, and 19 spectra were downloaded from the NARVAL and ESPaDOnS spectral archive PolarBase (Petit et al. 2014).

The FIES-spectra have $R \sim 67000$ and the PolarBase-spectra have $R \sim 65000$. They both cover the entire optical part of the spectrum, but only the region between 5800 Å and 6800 Å is used in the analysis, to be consistent with the analysis of the bulge spectra in Paper II.

Most of the stars observed are very bright, and have typical observing times of the order of minutes. The 213 stars observed by us using FIES were observed using the ‘exp-count’-feature, aborting the exposure when a specified CCD count-level have been reached. Therefore, a vast majority of these spectra have a S/N of 80-120, see Table 4 (Online material). The spectra downloaded from PolarBase generally have similar S/N, while the FIES-archive spectra generally have slightly higher S/N, while the spectra from Thygesen et al. (2012) have lower S/N, around 30-50. All S/N as measured by the IDL-routine `der_snr.pro`¹ are listed in Table 4 (Online material).

Our FIES-spectra were reduced using the standard FIES-pipeline, while the spectra from Thygesen et al. (2012) and PolarBase were already reduced and ready to analyze. All spectra have been roughly normalized using the IRAF task `continuum`. In the analysis-step a more careful continuum-normalization is made for every wavelength window analyzed (see Section 3).

No sky-subtraction and/or removal of telluric lines were attempted, instead regions of the spectra influenced by telluric absorption lines and bright sky emission lines were avoided: as can be seen in Figure 1, telluric lines are affecting regions around the stellar oxygen and magnesium lines, while only the stellar oxygen line is affected by a possible sky emission line. The telluric lines and sky-line affecting regions around the widely used 6300 Å oxygen line are important sources of uncertainties in the derived oxygen abundances in all works using this line.

The basic data for the analyzed disk giant stars are listed in Table 4 (Online material).

3. Analysis

The 291 local disk spectra analyzed in this paper, as well as the 46 bulge spectra analyzed in Paper II were analyzed in the exact same way to ensure a strictly differential comparison.

We used the software Spectroscopy Made Easy, SME (Valenti & Piskunov 1996). SME simultaneously fits stellar parameters and/or abundances by fitting calculated synthetic spectra to an observed spectrum using χ^2 -minimization. By selecting regions with spectral lines of interest and points which SME should treat as continuum points, specific lines can be chosen as basis of the analysis. Special care was taken to avoid fitting spectral regions affected by telluric lines, particularly a problem for the oxygen and magnesium lines used.

We have used spherical symmetric, $[\alpha/\text{Fe}]$ -enhanced, LTE MARCS-models in the analysis. Within the Gaia-ESO collab-

¹ See http://www.stecf.org/software/ASTROsoft/DER_SNR

oration (Gilmore et al. 2012) SME has been modified to apply NLTE departure coefficients interpolated from the grid presented by Lind et al. (2012), which covers the stellar parameters and lines used in the analysis.

We determine all the stellar parameters (T_{eff} , $\log g$, $[\text{Fe}/\text{H}]$, and ξ_{micro}) simultaneously, using relatively weak, unblended Fe I, Fe II, and Ca I lines and gravity-sensitive Ca I-wings (Edvardsson 1988). This means that the Ca-abundance is fitted simultaneously as the stellar parameters, but all other abundances are determined with fixed stellar parameters. The atomic data of the spectral lines used are listed in Table 5 (Online material).

3.1. Line data

All line-data used, in both determining the stellar parameters as well as the abundances, have been taken from version 5 of the Gaia-ESO line-list (Heiter et al. 2015b) with some exceptions: the wavelength-data of all Fe II-lines have been updated with values from Nave & Johansson (2013), and the $\log gf$ -values have been updated from the calculated values of Raassen & Uylings (1998) to the astrophysical values of Meléndez & Barbuy (2009). The latter values produce better fitting synthetic spectra, and most importantly, produce spectroscopic surface gravities closer to the asteroseismic surface gravities for the Kepler-stars in our sample. Furthermore the $\log gf$ -values of the three Mg I-lines used, have been updated from the calculated values of Butler et al. (1993) to values from Pehlivan et al. (in prep). There is an autoionizing Ca I-line close to these Mg I-lines producing a very wide (up to 5 Å) and shallow depression in the spectra. We found that removing this line from the synthesis, and instead placing a local continuum around Mg I-lines produced the tightest magnesium trend in our data. Therefore no atomic data for the autoionizing Ca I-line is used. Since we use the 6300.3083 Å [O I]-line to determine oxygen abundance, the atomic data of the blending Ni I-line at 6300.3419 Å is also of importance: here we have used the experimental $\log gf = -2.11$ from Johansson et al. (2003). In the analysis of the different stars, a solar Ni-abundance scaled with the iron abundance of that particular star was used.

The line data of the lines used is listed in Table 5 (Online material). The final line list consists of 47 lines, of which 39 are used to determine the stellar parameters and the Ca-abundance. All lines are situated in the wavelength range between 5800 Å to 6800 Å to match the usable range of the bulge spectra analyzed in Paper II, thereby enabling a strictly differential comparison.

Regarding the broadening of spectral lines due to collisions with neutral hydrogen (van der Waals broadening) the data for all the listed lines are taken from Barklem & Aspelund-Johansson (2005) and Barklem et al. (2000), with some exceptions not available in those references: for the Fe I line at 6793 Å values from Kurucz (2007) are used, for the Ca I line at 5867 Å values from Smith (1988) are used, for the 6300 Å [O I]-line values from Wiese et al. (1966) are used, and for the three Mg I-lines values from Kurucz & Peytremann (1975) are used.

To minimize the errors and uncertainties in the determined stellar parameters and abundances we have carefully checked all used lines for (known) blends in a grid of stellar atmospheres, using a similar method as was used in Jönsson et al. (2011). Typically a massive wealth of TiO molecular lines makes most lines in our wavelength range very hard to use for stars with temperatures below ~ 3900 K.

3.2. Random uncertainties in the stellar parameters

Random uncertainties in our method of determining the stellar parameters include both the freedom in setting the continuum and in the actual line fit. These obviously depend on the S/N of the observation in question. To test this, we have degraded the Arcturus spectrum of Hinkle et al. (2000) to different S/N and determined the stellar parameters for those spectra. The IDL-routine `x_addnoise`² was used to inject noise and create 100 realizations each of Arcturus-spectra with S/N of 10 to 120 in steps of 10. The parameters for these spectra were then derived exactly as for the science spectra, and the results are shown in the box-plots in Figure 2.

From Figure 2 one can deduce that for a $S/N \gtrsim 50$ the uncertainties are of the same order, while they grow very large for $S/N \lesssim 20$, meaning that integration times, at least for Arcturus-like stars, preferably should be adjusted to reach a $S/N > 20$, but do not have to be so long that a much greater S/N than 50 is reached. However cooler and/or more metal-rich stars likely need higher S/N to resolve the more numerous lines, and also higher S/N is desired when determining, for example, the oxygen abundance that is based on a single line (see Table 5, Online material). Of interest is also that it is mainly the ‘whiskers’ of the plots that are expanding for lower S/N, the ‘boxes’, holding 50% of the data, is more similarly sized as the S/N is lowered. This means that, even for the lowest S/N-bins, we are determining reasonable stellar parameters for a majority of the spectra.

Since all our program stars are bright, they have excellent S/N, in general around 100, and we can therefore, based on Figure 2, conclude that the random uncertainties stemming from the quality of the spectrum for an Arcturus-like red giant would be very small, of the order $\delta T_{\text{eff}} = \pm 10$ K, $\delta \log g = \pm 0.05$, $\delta [\text{Fe}/\text{H}] = \pm 0.02$, $\delta v_{\text{mic}} = \pm 0.02$ (standard deviation). Instead our uncertainties are dominated by the systematic uncertainties evaluated in the next section.

In Paper II, the uncertainties of the stellar parameters and abundances derived from the observations of the very faint bulge stars will in many cases be dominated by the random uncertainties stemming from the S/N.

3.3. Systematic uncertainties in the stellar parameters

Systematic uncertainties in stellar parameters and abundances are very hard to assess: they stem from everything from uncertainties in the atomic data used, to simplifications in the stellar atmosphere models. To assess these systematic uncertainties of the stellar parameters, we evaluate them in three steps by comparison with trusted benchmark values:

- In our sample, we have observed three of the giants of the Gaia-ESO benchmark stars (Heiter et al. 2015a; Jofré et al. 2014, 2015) with well determined parameters and abundances. Our results and the benchmark values are listed in Table 1.

For these three stars, we find our parameters to be within the uncertainties of the benchmark values with one exception: our $\log g$ for μ Leo is slightly higher. In general all our surface gravities are slightly higher than the three benchmark values, but for the other two stars our results are as stated within the uncertainties.

- Furthermore we note that, except for Arcturus, β Gem, and μ Leo, nine of our program stars have temper-

² <http://www.ucolick.org/~xavier/IDL/>

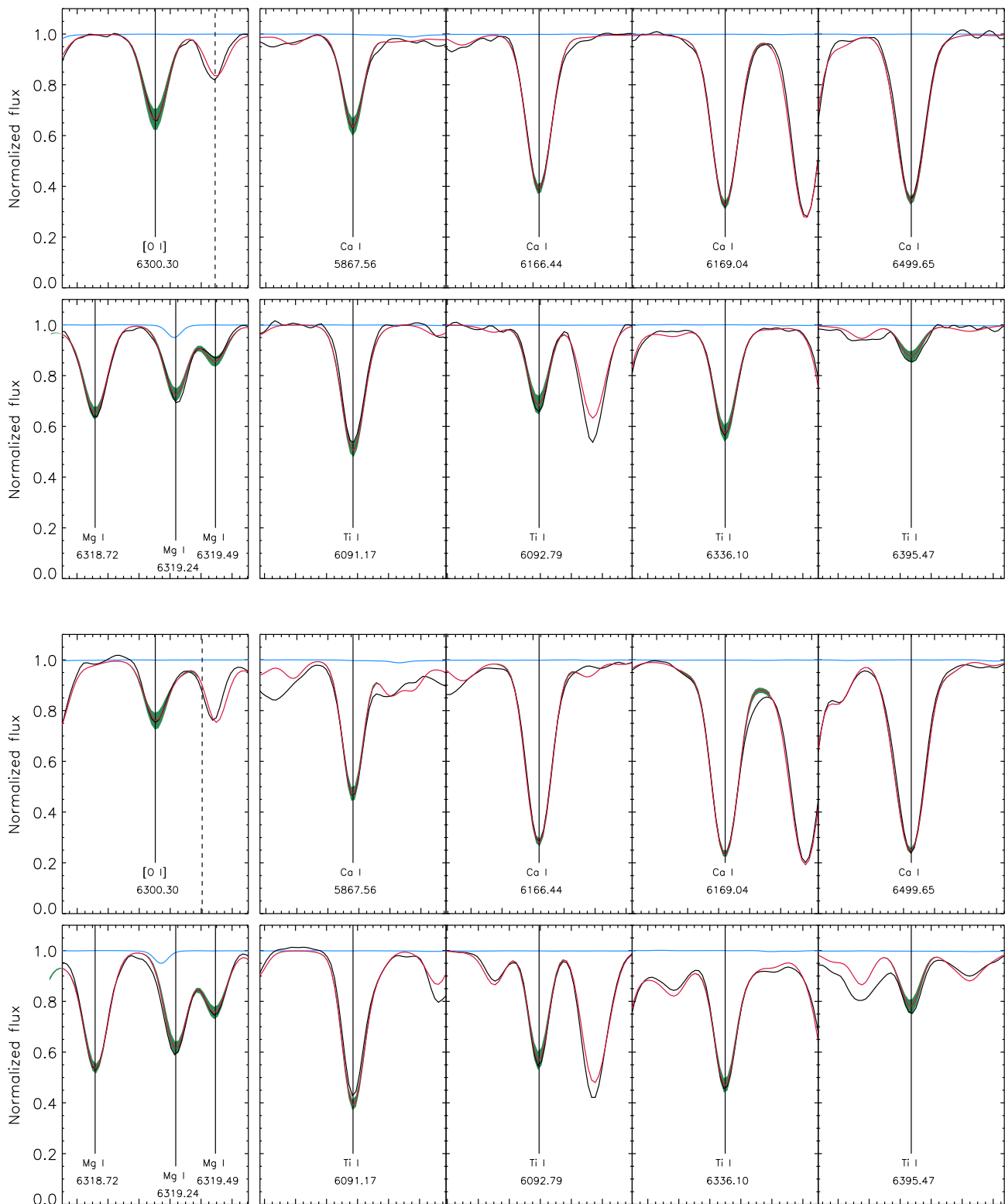


Fig. 1. The stellar lines used for abundance determinations in the analyzed FIES-spectra of Arcturus and μ Leo, in the top and bottom two rows respectively. The stellar spectrum is shown in black, the best fitting synthetic spectrum in red, and ± 0.1 dex of the element in question in green. The telluric spectrum from the Arcturus atlas of Hinkle et al. (2000) is shown in blue and the position of the bright 6300 Å sky emission line is shown using a dashed line. Stellar lines possibly affected by telluric absorption lines and/or sky emission lines were avoided in the analysis. All panels show 1.2 Å of spectra surrounding the line in question, i.e. the larger tickmarks mark steps of 0.2 Å.

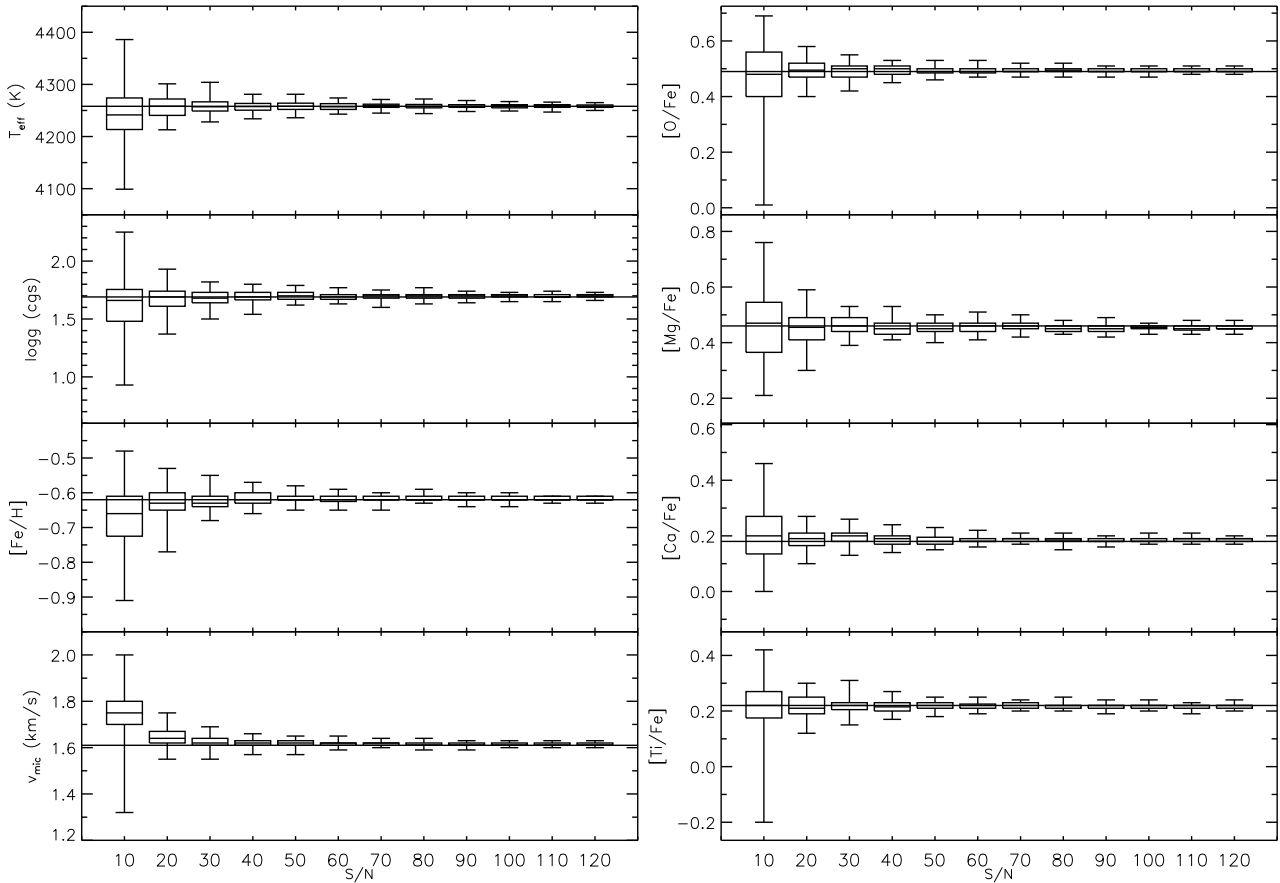


Fig. 2. Results from determining the stellar parameters and abundances for Arcturus spectra with different injected S/N. The horizontal line crossing each panel represents the value as determined from the original, high-S/N, atlas spectrum. The horizontal line in the boxes shows the median of the data, the lower and upper boundaries of the boxes show the lower and upper quartiles of the data, and the whiskers extend to the lowest and highest value of the data.

Table 1. The Gaia-ESO stellar parameter benchmark values (Heiter et al. 2015a; Jofré et al. 2014, 2015) are listed for the three giants in our sample. On the row below are the stellar values determined using our analysis for the corresponding star. In the case of Arcturus (HIP68673), we have two determinations: the first row shows our results using our FIES-spectrum, and the second row shows our results using the atlas of Hinkle et al. (2000). [Fe/H] is listed in the (Asplund et al. 2009) scale, i.e. with $A(\text{Fe})_{\odot} = 7.50$

HIP	Name	T_{eff}	$\log g$	[Fe/H]	v_{mic}	A(O)	A(Mg)	A(Ca)	A(Ti)
HIP37826	β Gem	4858 ± 60	2.90 ± 0.08	0.08 ± 0.16	1.28 ± 0.21	...	7.56 ± 0.07	6.40 ± 0.08	4.96 ± 0.07
		4835	2.93	0.04	1.24	8.69	7.63	6.43	4.92
HIP48455	μ Leo	4474 ± 60	2.51 ± 0.11	0.20 ± 0.15	1.28 ± 0.26	...	8.11 ± 0.11	6.60 ± 0.12	5.22 ± 0.10
		4461	2.65	0.20	1.55	8.93	7.83	6.50	5.13
HIP69673	α Boo	4286 ± 35	1.64 ± 0.09	-0.57 ± 0.08	1.58 ± 0.12	...	7.49 ± 0.09	5.92 ± 0.13	4.59 ± 0.08
		4251	1.72	-0.60	1.64	8.57	7.38	5.88	4.54
		4258	1.69	-0.62	1.61	8.56	7.44	5.91	4.55

atures determined from angular diameter measurements (Mozurkewich et al. 2003), see Table 2.

Our determined temperatures are within the uncertainties from the temperatures of Mozurkewich et al. (2003), with one exception: β UMi, where we derive a temperature 143 K higher than the reference value, showing the difficulties in determining the temperatures for the very coolest stars. All in all, we are able to derive the temperatures of these stars with a systematic offset of +10 K and a standard deviation

of 53 K, very similar to the mean of the uncertainties of the measurements of Mozurkewich et al. (2003): 56 K.

- When it comes to the surface gravity, our sample includes 39 giants in the Kepler field with asteroseismic gravities (Thygesen et al. 2012; Huber et al. 2014): our determined gravities are deviating from the seismic values with a systematic offset of +0.10 dex and a standard deviation of 0.12 dex.

Table 2. The effective temperatures as derived based on angular diameter measurements (Mozurkewich et al. 2003) listed for the nine giants in our sample. Also listed are the stellar parameters determined using our analysis based on observations from a FIES, NARVAL, or ESPOONS spectrum for the corresponding star.

HIP	Name	$T_{\text{eff,ref}}$	T_{eff}	$\log g$	[Fe/H]
HIP9884	α Ari	4493 \pm 55	4464	2.27	-0.24
HIP46390	α Hya	4060 \pm 50	4095	1.56	-0.10
HIP54539	ψ UMa	4550 \pm 56	4534	2.33	-0.10
HIP55219	ν UMa	4091 \pm 50	4133	1.65	-0.17
HIP72607	β UMi	3849 \pm 47	3992	1.32	-0.23
HIP74666	δ Boo	4850 \pm 60	4861	2.63	-0.37
HIP77070	α Ser	4558 \pm 56	4540	2.61	0.16
HIP94376	δ Dra	4851 \pm 67	4807	2.71	-0.17
HIP102488	ϵ Cyg	4756 \pm 59	4711	2.59	-0.18

To conclude, our determined effective temperatures seem very precise with a systematic shift of only +10 K, while we likely have a systematic shift of +0.1 dex in surface gravity. Regarding the metallicity, we only have three benchmark values, but our results are accurate with respect to those.

3.4. Uncertainties in the determined abundances

When it comes to the uncertainties in the determined abundances, we assess and estimate them below in three steps:

- In the rightmost panels of Figure 2, we show the determined abundances in the S/N-injected spectra, using the stellar parameters as determined in the same S/N-injected spectrum (those that are shown in the leftmost panels). As expected, the uncertainties in the determined abundances follow the uncertainties in the stellar parameters, and show very large uncertainties for the lowest S/N-bin. However, just like for the stellar parameters, the box, holding 50% of the values is still reasonably small, meaning that we still derive acceptable abundances for a majority of the spectra. Based on this investigation, the influence of S/N of the determined abundances of the high-S/N stars in this paper, is negligible, but it might be significant for some of the bulge spectra of Paper II having S/N < 20.
- In Table 1 in addition to the stellar parameters, also list the abundances of the three stars overlapping between Heiter et al. (2015a); Jofré et al. (2014, 2015) and our sample. Our abundances fall within the uncertainties of the benchmark values with one obvious and one more subtle exception. Firstly, our derived magnesium abundance of μ Leo is much lower, than the value from Jofré et al. (2015). We cannot find any reason for this, but note that the benchmark value would place μ Leo significantly above the [Mg/Fe] vs. [Fe/H] trend if Figure 4 at ([Fe/H];[Mg/Fe]) = (0.20; 0.31), while our result is more following the rest of the disk stars with ([Fe/H];[Mg/Fe]) = (0.20; 0.03). Secondly, our magnesium abundance as derived from the FIES-spectrum of Arcturus is also slightly lower than the benchmark value including its uncertainty. The abundance as derived from the Hinkle et al. (2000) atlas spectrum, however, is within the uncertainties of the benchmark value. The magnesium abundances as derived from the FIES-spectrum and the atlas-spectrum are deviating more than the abundances of oxygen, calcium, and titanium. Since the magnesium lines, as described in Section 3.1, have a neighboring autoionizing line whose curving influence on the continuum is hard to get

rid of, it is not unexpected for the magnesium abundance of these high-S/N spectra to show higher uncertainty than the other abundances.

- The uncertainties of determined abundances are often dominated by the uncertainties of the stellar parameters, and as is suggested by the similar shapes of the parameter-boxes and the abundance-boxes in Figure 2, so is likely the case in this study. To estimate these uncertainties, often a table like Table 3 is used. This table is best used as a way of telling

Table 3. The uncertainties of the derived abundances of a typical star (our FIES Arcturus spectrum) for changes in the derived stellar parameters.

Uncertainty	$\delta A(\text{O})$	$\delta A(\text{Mg})$	$\delta A(\text{Ti})$
$\delta T_{\text{eff}} = -50$ K	-0.01	+0.01	-0.07
$\delta T_{\text{eff}} = +50$ K	+0.01	± 0.00	+0.07
$\delta \log g = -0.15$	-0.07	-0.02	-0.01
$\delta \log g = +0.15$	+0.06	+0.03	+0.01
$\delta [\text{Fe}/\text{H}] = -0.05$	+0.02	± 0.00	± 0.00
$\delta [\text{Fe}/\text{H}] = +0.05$	-0.01	± 0.00	± 0.00
$\delta v_{\text{mic}} = -0.1$	± 0.00	0.01	+0.02
$\delta v_{\text{mic}} = +0.1$	-0.01	-0.01	-0.02

which abundances are most uncertain, and which parameter is mainly influencing the different abundances. For example, our probable systematic error of +0.1 dex in determining the $\log g$ is mainly going to influence the oxygen abundance, while the titanium abundance is not affected by this. Estimating the total uncertainty in the abundance determination by adding the different uncertainties in quadrature would overestimate the uncertainties, since the parameters are coupled and deriving an incorrect temperature possibly would lead to an incorrect metallicity, for example. Furthermore, such an exercise would be based on the uncertainties of the stellar parameters which in themselves are hard to estimate (compare Section 3.2).

To conclude we can estimate expected typical uncertainties of the determined abundances to be almost of the order of 0.1 dex for magnesium, and likely lower for the others.

4. Results

The HR-diagram based on the spectroscopically determined stellar parameters of the observed giants are shown in Figure 3. Also shown in the figure are the 604 solar neighborhood dwarf stars of Bensby et al. (2014) with $T_{\text{eff}} > 5400$ K and a collection of isochrones (Bressan et al. 2012).

Our derived abundances for the giants can be seen in Table 6 (Online material) and in Figure 4. As a comparison, the corresponding abundances as derived in a local disk sample of dwarf stars by Bensby et al. (2014) is also shown in the figure.

5. Discussion

The aim of this analysis is twofold: to find as accurate stellar parameters and abundances as possible from giants, but most importantly, to collect a sample of homogeneously analyzed Solar neighborhood targets similar to the bulge targets that will be presented in Paper II. The second aim means that we have to restrict our present analysis to the wavelength coverage of the bulge spectra even if the spectra analyzed here have a wider coverage. In turn, this optional restriction might lead to a possibly lower

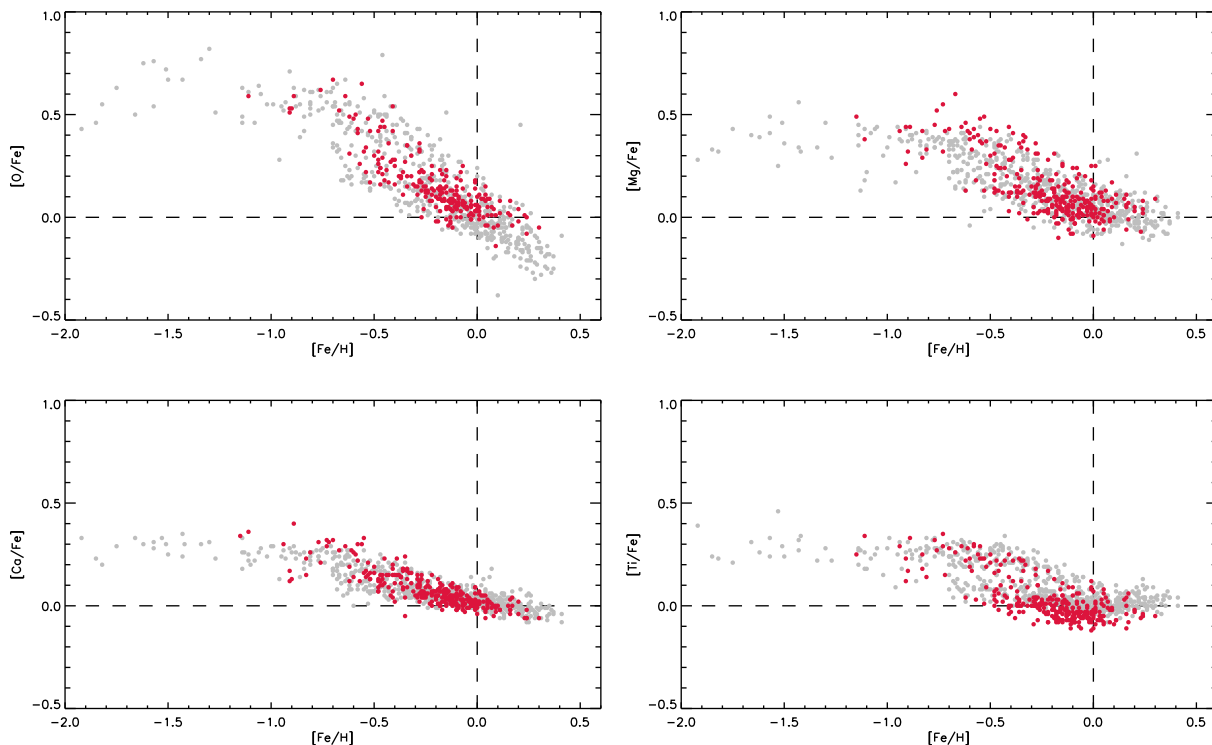


Fig. 4. $[X/Fe]$ for the observed giants in red, compared to abundances of the 604 solar neighborhood dwarf stars of Bensby et al. (2014) with $T_{\text{eff}} > 5400$ K in gray. Especially for O and Ti a clear separation of thin and thick disk type abundances can be seen in our sample. Since our sample is mostly made up of the very brightest, closest, giants, it is not surprising that a majority of the stars show thin disk type chemistry. In the plots we use $A(O)_{\odot} = 8.69$, $A(Mg)_{\odot} = 7.60$, $A(Ca)_{\odot} = 6.34$, $A(Ti)_{\odot} = 4.95$, and $A(Fe)_{\odot} = 7.50$ (Asplund et al. 2009).

precision of the abundances in the Solar neighborhood sample that what would have been possible to attain using the entire coverage available from FIES, NARVAL, and ESPaDOnS.

The low deviations of the temperatures and gravities determined when compared to the more accurate angular diameter and asteroseismic measurements, together with the alignment in of the measurements along the red giant branch and spread in $[Fe/H]$ in the HR-diagram (Figure 3), give us assurance that the method used likely is finding accurate values for the stellar parameters.

Estimating the formal uncertainties in abundance determinations is difficult: in our case where we have very high S/N-spectra and we are only using spectral lines with precise atomic data that are believed to be unblended, the main uncertainty of the abundances comes from the uncertainties of the stellar parameters. As elaborated on in Section 3.4, the often used way of adding the dependencies of the abundances on the individual stellar parameters (Table 3), gives an overestimation on the total abundance uncertainty. All in all, our results are showing very similar trends as the carefully analyzed dwarfs in Bensby et al. (2014) in Figure 4, and also have similarly tight trends, which hints at high precision in our derived abundances. The mean of the uncertainties quoted in Bensby et al. (2014) for the 604 stars with $T_{\text{eff}} > 5400$ K are $\delta A(O) \sim 0.14$, $\delta A(Mg) \sim 0.06$, $\delta A(Ca) \sim 0.06$, $\delta A(Ti) \sim 0.07$, and our uncertainties are thus likely at the same order. In the case of magnesium our scatter is higher, hinting at a larger uncertainty, but in the case of oxygen our trend looks tighter, hinting at lower mean uncertainty than that of Bensby et al. (2014). This is not unexpected, since

Bensby et al. use the very NLTE-sensitive oxygen triplet around $7771\text{-}7775$ Å (Amarsi et al. 2016), although with corrections, making their oxygen abundances less precise than their other abundances, a fact that is reflected in their higher quoted uncertainty for oxygen as mentioned above.

Based on the comparison between our abundance trends using K-giants and those of the carefully analyzed dwarfs of Bensby et al. (2014) we would like to claim that giant stars are as good as abundance indicators as dwarfs. This is an important point, since this opens up the usefulness of the giants due to their brightness. However, as described in Section 1, care must be shown to possible blending lines, continuum fitting, and the atomic and/or molecular data for the used spectral lines.

6. Conclusions

The main purpose of this paper is to analyze a sample of local disk K-giants to be used as a comparison sample for the similar sample bulge giants to be analyzed in Paper II. To be sure the local sample can be strictly differentially compared to the bulge sample, where photometry is difficult/uncertain, we have chosen a strictly spectroscopic approach. Furthermore we have chosen to restrict our analysis to the useful part of the bulge spectra: 5800 Å– 6800 Å. When we compare the determined effective temperatures to those derived from angular diameter measurements, we reproduce these with a systematic difference of $+10$ K and a standard deviation of 53 K. The spectroscopic gravities are reproducing the ones determined from asteroseismology with a systematic offset of $+0.10$ dex and a standard deviation of

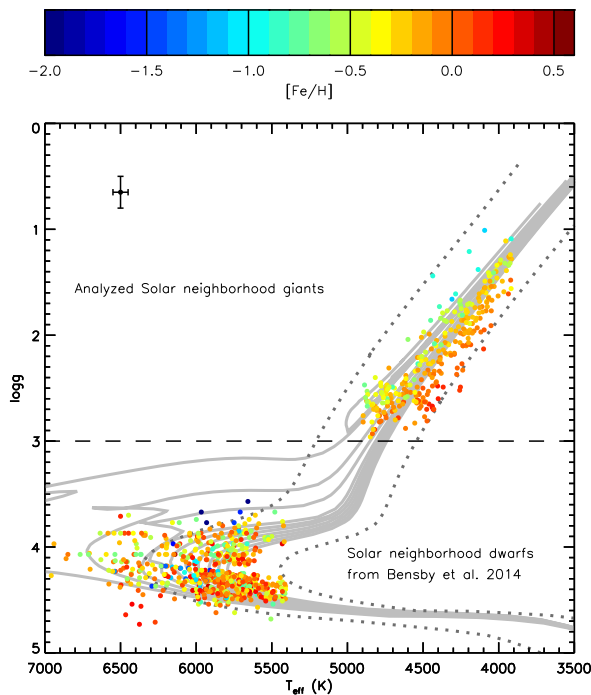


Fig. 3. HR-diagrams for the observed giants and the 604 Solar neighborhood dwarfs of Bensby et al. (2014) with $T_{\text{eff}} > 5400$ K. As a guide for the eye, isochrones with $[\text{Fe}/\text{H}]=0.0$ and ages 1-10 Gyr are plotted using solid light gray lines. Furthermore, one isochrone with $[\text{Fe}/\text{H}]=-1.0$ and age 10 Gyr, and one with $[\text{Fe}/\text{H}]=+0.5$ and age 10 Gyr are plotted using dotted dark grey lines (Bressan et al. 2012). The parameters of the analyzed giants are determined from spectroscopy as described in the text. They line up as expected from isochrones in both temperature, and surface gravity, as well as metallicity. Expected, typical uncertainties are marked in the top left corner of the plot.

0.12 dex. Regarding the abundance trends, our sample of local disk giants is closely following that of the Solar neighborhood dwarfs of Bensby et al. (2014) with similar spread and no obvious systematic differences.

Ideally, our sample should have consisted of more stars with typical thick disk abundances to better represent both local disk stellar populations, and we plan to expand the sample accordingly in the near future.

Acknowledgements. Anders Thygesen is thanked for offering the reduced spectra of their stars online, and for kindly providing the observation dates/times to enable a scan for telluric contamination. John Telting is thanked for help with the FIES-data, and in particular archive-data. This research has been partly supported by the Lars Hierta Memorial Foundation, and the Royal Physiographic Society in Lund through Stiftelsen Walter Gyllenbergs fond and Märta och Erik Holmbergs donation. H.H., P.J., and N.R. acknowledges support from the Swedish Research Council, VR (project numbers 2011-4206, 2014-5640, and 2015-4842). This publication made use of the SIMBAD database, operated at CDS, Strasbourg, France, NASA's Astrophysics Data System, and the VALD database, operated at Uppsala University, the Institute of Astronomy RAS in Moscow, and the University of Vienna.

References

Aldenius, M., Lundberg, H., & Blackwell-Whitehead, R. 2009, *A&A*, 502, 989
 Alves-Brito, A., Meléndez, J., Asplund, M., Ramírez, I., & Yong, D. 2010, *Astronomy & Astrophysics*, 513, 35
 Amarsi, A. M., Asplund, M., Collet, R., & Leenaerts, J. 2016, *Monthly Notices of the Royal Astronomical Society*, 455, 3735

Asplund, M., Grevesse, N., Sauval, A. J., & Scott, P. 2009, *Annual Review of Astronomy and Astrophysics*, 47, 481
 Barbuy, B., Hill, V., Zoccali, M., et al. 2013, *Astronomy & Astrophysics*, 559, 5
 Bard, A., Kock, A., & Kock, M. 1991, *Astron. and Astrophys.*, 248, 315, (BKK)
 Bard, A. & Kock, M. 1994, *Astron. and Astrophys.*, 282, 1014, (BK)
 Barklem, P. S. & Asplund-Johansson, J. 2005, *Astron. and Astrophys.*, 435, 373, (BA-J)
 Barklem, P. S., Piskunov, N., & O'Mara, B. J. 2000, *Astron. and Astrophys. Suppl. Ser.*, 142, 467, (BPM)
 Bensby, T., Feltzing, S., & Oey, M. S. 2014, *Astronomy & Astrophysics*, 562, 71
 Bensby, T., Yee, J. C., Feltzing, S., et al. 2013, *Astronomy & Astrophysics*, 549, 147
 Blackwell, D. E., Booth, A. J., Menon, S. L. R., & Petford, A. D. 1986, *MNRAS*, 220, 289
 Blackwell, D. E., Petford, A. D., Shallis, M. J., & Simmons, G. J. 1982a, *MNRAS*, 199, 43
 Blackwell, D. E., Petford, A. D., & Simmons, G. J. 1982b, *MNRAS*, 201, 595
 Bressan, A., Marigo, P., Girardi, L., et al. 2012, *Monthly Notices of the Royal Astronomical Society*, 427, 127
 Butler, K., Mendoza, C., & Zeippen, C. J. 1993, *Journal of Physics B - Atomic*, 26, 4409
 Den Hartog, E. A., Ruffoni, M. P., Lawler, J. E., et al. 2014, *ArXiv e-prints*
 Di Matteo, P. 2016, *arXiv.org*, arXiv:1603.05485
 Edvardsson, B. 1988, *Astronomy and Astrophysics*, 190, 148
 Froese Fischer, C. & Tachiev, G. 2012, *Multiconfiguration Hartree-Fock and Multiconfiguration Dirac-Hartree-Fock Collection, Version 2*, available online at <http://physics.nist.gov/mchf/>
 Fuhr, J. R., Martin, G. A., & Wiese, W. L. 1988, *Journal of Physical and Chemical Reference Data*, Volume 17, Suppl. 4. New York: American Institute of Physics (AIP) and American Chemical Society, 1988, 17, (FMW)
 Gilmore, G., Randich, S., Asplund, M., et al. 2012, *The Messenger*, 147, 25
 Gonzalez, O. A. & Gadotti, D. A. 2015, *arXiv.org*, 7252
 González, O. A., Rejkuba, M., Zoccali, M., et al. 2011, *Astronomy & Astrophysics*, 530, 54
 Heiter, U., Jofré, P., Gustafsson, B., et al. 2015a, *Astronomy & Astrophysics*, 582, A49
 Heiter, U., Lind, K., Asplund, M., et al. 2015b, *Physica Scripta*, 90, 054010
 Hinkle, K., Wallace, L., Valenti, J., & Harmer, D. 2000, *Visible and Near Infrared Atlas of the Arcturus Spectrum 3727-9300 Å*
 Huber, D., Silva Aguirre, V., Matthews, J. M., et al. 2014, *The Astrophysical Journal Supplement*, 211, 2
 Jofré, P., Heiter, U., Soubiran, C., et al. 2015, *Astronomy & Astrophysics*, 582, A81
 Jofré, P., Heiter, U., Soubiran, C., et al. 2014, *Astronomy & Astrophysics*, 564, A133
 Johansson, S., Litzén, U., Lundberg, H., & Zhang, Z. 2003, *ApJ*, 584, L107
 Johnson, C. I., McWilliam, A., & Rich, R. M. 2013, *The Astrophysical Journal Letters*, 775, L27
 Johnson, C. I., Rich, R. M., Kobayashi, C., & Fulbright, J. P. 2012, *The Astrophysical Journal*, 749, 175
 Johnson, C. I., Rich, R. M., Kobayashi, C., Kunder, A., & Koch, A. 2014, *The Astronomical Journal*, 148, 67
 Jönsson, H., Ryde, N., Nissen, P. E., et al. 2011, *Astronomy & Astrophysics*, 530, 144
 Kurucz, R. L. 2007, Robert L. Kurucz on-line database of observed and predicted atomic transitions
 Kurucz, R. L. 2013, Robert L. Kurucz on-line database of observed and predicted atomic transitions
 Kurucz, R. L. & Peytremann, E. 1975, *SAO Special Report*, 362, 1, (KP)
 Lacy, J. H., Richter, M. J., Greathouse, T. K., Jaffe, D. T., & Zhu, Q. 2002, *The Publications of the Astronomical Society of the Pacific*, 114, 153
 Lawler, J. E., Guzman, A., Wood, M. P., Sneden, C., & Cowan, J. J. 2013a, *ApJS*, 205, 11
 Lawler, J. E., Guzman, A., Wood, M. P., Sneden, C., & Cowan, J. J. 2013b, *ApJS*, 205, 11
 Lecureur, A., Hill, V., Zoccali, M., et al. 2007, *Astronomy & Astrophysics*, 465, 799
 Lind, K., Bergemann, M., & Asplund, M. 2012, *Monthly Notices of the Royal Astronomical Society*, 427, 50
 May, M., Richter, J., & Wichelmann, J. 1974, *A&AS*, 18, 405, (MRW)
 Meléndez, J. & Barbuy, B. 2009, *Astronomy & Astrophysics*, 497, 611
 Mozurkewich, D., Armstrong, J. T., Hindsley, R. B., et al. 2003, *The Astronomical Journal*, 126, 2502
 Nave, G. & Johansson, S. 2013, *The Astrophysical Journal Supplement*, 204, 1
 O'Brian, T. R., Wickliffe, M. E., Lawler, J. E., Whaling, W., & Brault, J. W. 1991, *Journal of the Optical Society of America B Optical Physics*, 8, 1185, (BWL)
 Petit, P., Louge, T., Théado, S., et al. 2014, *Publications of the Astronomical Society of the Pacific*, 126, 469

- Raassen, A. J. J. & Uylings, P. H. M. 1998, *A&A*, 340, 300, (RU)
- Ralchenko, Y., Kramida, A., Reader, J., & NIST ASD Team. 2010, NIST Atomic Spectra Database (ver. 4.0.0), [Online].
- Rich, R. M. 2013, *Planets*, 271
- Ruffoni, M. P., Den Hartog, E. A., Lawler, J. E., et al. 2014, *Monthly Notices of the Royal Astronomical Society*, 441, 3127
- Ryde, N., Gustafsson, B., Edvardsson, B., et al. 2010, *Astronomy & Astrophysics*, 509, 20
- Smith, G. 1981, *Astron. and Astrophys.*, 103, 351, (Sm)
- Smith, G. 1988, *Journal of Physics B Atomic Molecular Physics*, 21, 2827, (S)
- Smith, G. & O'Neill, J. A. 1975, *Astron. and Astrophys.*, 38, 1, (SN)
- Smith, G. & Raggett, D. S. J. 1981, *Journal of Physics B Atomic Molecular Physics*, 14, 4015, (SR)
- Storey, P. J. & Zeippen, C. J. 2000, *Monthly Notices of the Royal Astronomical Society*, 312, 813
- Telting, J. H., Avila, G., Buchhave, L., et al. 2014, *Astronomische Nachrichten*, 335, 41
- Thygesen, A. O., Frandsen, S., Bruntt, H., et al. 2012, *Astronomy & Astrophysics*, 543, 160
- Valenti, J. A. & Piskunov, N. 1996, *Astronomy and Astrophysics Supplement*, 118, 595
- Van der Swaelmen, M., Barbuy, B., Hill, V., et al. 2016, *Astronomy & Astrophysics*, 586, A1
- Wiese, W. L., Smith, M. W., & Glennon, B. M. 1966, *Atomic transition probabilities. Vol.: Hydrogen through Neon. A critical data compilation*, ed. Wiese, W. L., Smith, M. W., & Glennon, B. M. (US Government Printing Office), (WSG)
- Zoccali, M., Lecqueur, A., Barbuy, B., et al. 2006, *Astronomy & Astrophysics*, 457, L1

Table 4. Basic data for the observed giants. Coordinates and magnitudes are taken from the SIMBAD database, while the radial velocities are measured from the spectra. The S/N per datapoint is measured by the IDL-routine `der_snr.pro`, see http://www.stecf.org/software/ASTROsoft/DER_SNR.

HIP/KIC/TYC	Alternative name	RA (J2000) (h:m:s)	Dec (J2000) (d:am:as)	<i>V</i>	<i>v</i> _{rad} km/s	S/N	Source
HIP1692	HD1690	00:21:13.32713	-08:16:52.1625	9.18	18.37	114	FIES-archive
HIP9884	alfAri	02:07:10.40570	+23:27:44.7032	2.01	-14.29	90	PolarBase
HIP10085	HD13189	02:09:40.17260	+32:18:59.1649	7.56	26.21	156	FIES-archive
HIP12247	81Cet	02:37:41.80105	-03:23:46.2201	5.66	9.34	176	FIES-archive
HIP28417	HD40460	06:00:06.03883	+27:16:19.8614	6.62	100.64	121	PolarBase
HIP33827	HR2581	07:01:21.41827	+70:48:29.8674	5.69	-17.99	79	PolarBase
HIP35759	HD57470	07:22:33.85798	+29:49:27.6626	7.67	-30.19	85	PolarBase
HIP37447	alfMon	07:41:14.83257	-09:33:04.0711	3.93	11.83	71	Thygesen et al. (2012)
HIP37826	betGem	07:45:18.94987	+28:01:34.3160	1.14	3.83	90	PolarBase
HIP43813	zetHya	08:55:23.62614	+05:56:44.0354	3.10	23.37	147	PolarBase
HIP46390	alfHya	09:27:35.24270	-08:39:30.9583	1.97	-4.28	54	PolarBase
HIP48455	muLeo	09:52:45.81654	+26:00:25.0319	3.88	13.19	89	FIES-archive
HIP50583	gamLeo	10:19:58.35056	+19:50:29.3468	2.37	-35.45	142	FIES-prg 51-018
HIP52943	nuHya	10:49:37.48875	-16:11:37.1360	3.11	2.10	118	PolarBase
HIP53740	alfCrt	10:59:46.46486	-18:17:55.6172	4.07	47.42	119	PolarBase
HIP54539	psiUMa	11:09:39.80868	+44:29:54.5520	3.01	-3.34	117	FIES-prg 51-018
HIP55219	nuUMa	11:18:28.73664	+33:05:39.5107	3.49	-8.95	127	FIES-prg 51-018
HIP57477	HD102328	11:46:55.62214	+55:37:41.4853	5.26	1.13	79	FIES-prg 51-018
HIP58628	HD104406	12:01:23.57197	+25:42:59.0303	9.02	-9.48	95	FIES-prg 51-018
HIP63432	9Dra	12:59:55.07055	+66:35:50.1693	5.38	-32.52	140	FIES-prg 51-018
HIP64022	41Com	13:07:10.73003	+27:37:29.0585	4.69	-15.12	95	FIES-prg 51-018
HIP65028	HD115927	13:19:47.26850	+36:22:26.0912	7.70	2.68	92	PolarBase
HIP66726	BD+402678	13:40:39.94088	+39:43:45.1907	9.60	3.92	106	FIES-prg 53-002
HIP66900	BD+282252	13:42:35.23057	+27:16:16.6084	9.70	4.97	105	FIES-prg 53-002
HIP67608	HD120802	13:51:12.05161	+27:07:43.6725	8.19	-21.68	80	PolarBase
HIP68501	HD122456	14:01:22.31828	+31:33:48.9557	6.88	-29.62	100	FIES-prg 51-018
HIP68567	HR5271	14:02:12.18859	+45:45:12.4455	6.28	-49.66	100	FIES-prg 51-018
HIP68739	HR5276	14:04:14.56119	-05:22:53.1070	6.40	-9.86	80	FIES-prg 53-002
HIP68763	HR5277	14:04:26.98048	-14:58:18.1373	6.35	-13.42	109	FIES-prg 53-002
HIP68932	HD123518	14:06:41.26759	+53:18:44.2969	7.12	-17.59	111	FIES-prg 53-002
HIP68955	HD123409	14:06:55.82865	+28:26:16.9555	6.89	-56.32	124	FIES-prg 53-002
HIP69067	HD123612	14:08:15.86018	+24:18:54.1804	6.56	-26.31	93	FIES-prg 51-018
HIP69107	HR5302	14:08:46.04616	+59:20:15.5342	6.47	7.89	119	FIES-prg 53-002
HIP69118	HD123783	14:08:54.86377	+32:01:08.2385	8.16	3.19	90	FIES-prg 51-018
HIP69127	96Vir	14:09:00.59357	-10:20:04.3689	6.46	-15.19	121	FIES-prg 53-002
HIP69198	HD124018	14:09:59.72173	+40:46:41.5481	7.15	-14.30	89	FIES-prg 53-002
HIP69253	BD+402745	14:10:36.77038	+39:25:39.5430	8.89	23.86	87	FIES-prg 51-018
HIP69295	HD124319	14:11:01.35953	+58:32:56.3639	6.74	-14.03	130	FIES-prg 51-018
HIP69316	HR5310	14:11:15.12108	+32:17:45.2102	6.14	-20.12	81	FIES-prg 51-018
HIP69585	HD124678	14:14:35.60611	+13:58:31.6170	6.44	-15.06	95	FIES-prg 53-002
HIP69612	15Boo	14:14:50.85024	+10:06:02.1964	5.29	17.26	119	FIES-prg 51-018
HIP69673	alfBoo	14:15:39.67207	+19:10:56.6730	-0.05	-5.16	117	FIES-archive
HIP70548	HD126598	14:25:54.58205	+26:15:54.9601	7.44	3.92	87	FIES-prg 51-018
HIP70899	HD127227	14:29:53.68830	+16:12:31.5485	7.53	-39.85	69	FIES-prg 51-018
HIP70949	HD127337	14:30:45.38986	+04:46:20.2374	6.02	7.36	108	FIES-prg 51-018
HIP71568	HR5464	14:38:12.58863	+43:38:31.6693	5.74	-49.99	126	FIES-prg 51-018
HIP71996	HD129845	14:43:25.75736	+45:45:40.7462	9.63	-9.70	120	FIES-prg 53-002
HIP72012	HR5493	14:43:44.43396	+40:27:33.3156	5.73	12.07	112	FIES-prg 51-018
HIP72462	HD130686	14:49:02.45221	+19:20:51.6197	8.41	-13.21	95	FIES-prg 51-018
HIP72499	HD130705	14:49:26.15549	+10:02:38.9659	6.64	-28.73	73	FIES-prg 51-018
HIP72607	betUMi	14:50:42.32580	+74:09:19.8142	2.08	16.58	71	PolarBase
HIP72664	HD131507	14:51:26.43638	+59:17:38.3560	5.49	10.19	93	FIES-prg 53-002
HIP73203	HD132304	14:57:41.58372	+24:40:26.7824	6.95	-42.31	114	FIES-prg 51-018
HIP73388	HD132737	14:59:52.39237	+27:09:37.0352	7.63	-23.20	53	FIES-archive
HIP73568	omeBoo	15:02:06.50855	+25:00:29.3003	4.81	13.11	96	FIES-prg 51-018
HIP73745	psiBoo	15:04:26.74234	+26:56:51.5399	4.55	-25.48	114	FIES-prg 53-002
HIP73909	HR5635	15:06:16.71796	+54:33:22.7420	5.25	15.73	141	FIES-prg 51-018
HIP73917	HD133922	15:06:21.01070	+26:26:13.7376	7.90	3.40	94	FIES-prg 51-018

Table 4. Continued.

HIP/KIC/TYC	Alternative name	RA (J2000) (h:m:s)	Dec (J2000) (d:am:as)	V	v_{rad} km/s	S/N	Source
HIP73991	HD134063	15:07:15.44054	+22:33:51.6953	7.80	-112.30	138	FIES-prg 51-018
HIP74649	3Ser	15:15:11.35199	+04:56:21.7099	5.34	-33.61	105	FIES-prg 51-018
HIP74666	delBoo	15:15:30.16295	+33:18:53.3926	3.49	-11.95	174	FIES-prg 51-018
HIP75119	6Ser	15:21:01.99609	+00:42:55.2213	5.38	10.09	105	FIES-prg 51-018
HIP75127	HD136479	15:21:07.60862	-05:49:29.4630	5.54	-31.56	88	PolarBase
HIP75260	HR5737	15:22:38.41426	+63:20:29.1830	5.73	-43.83	83	FIES-prg 53-002
HIP75369	HR5732	15:24:05.11673	+45:16:15.7189	6.06	-11.06	100	FIES-prg 51-018
HIP75541	HD137719	15:25:59.08502	+44:18:08.0637	7.17	-9.11	96	FIES-prg 51-018
HIP75572	HR5741	15:26:17.38405	+34:20:09.5831	5.47	-48.75	114	FIES-prg 51-018
HIP75583	HD137688	15:26:30.15250	+28:07:39.0940	7.47	23.69	112	FIES-prg 51-018
HIP75822	HR5768	15:29:21.09415	+62:05:58.3063	6.29	-39.49	93	FIES-prg 53-002
HIP76333	gamLib	15:35:31.57881	-14:47:22.3278	3.91	-26.42	115	FIES-prg 53-002
HIP76634	HD139622	15:39:01.03721	+03:28:03.6523	7.34	-60.40	72	FIES-prg 51-018
HIP77070	alfSer	15:44:16.07431	+06:25:32.2633	2.63	3.17	48	PolarBase
HIP77578	omeSer	15:50:17.54635	+02:11:47.4362	5.23	-3.65	133	FIES-prg 51-018
HIP77743	HD142209	15:52:21.51136	+28:36:26.6294	7.91	-22.67	88	FIES-prg 51-018
HIP77748	HD142243	15:52:30.86222	+28:54:47.8879	7.80	-26.24	95	FIES-prg 51-018
HIP78132	phiSer	15:57:14.57093	+14:24:52.1359	5.55	-70.44	106	FIES-prg 51-018
HIP78157	HD143064	15:57:33.74407	+16:04:21.6363	8.49	27.58	80	FIES-prg 51-018
HIP78262	HD143257	15:58:49.08346	+16:12:39.9000	7.71	-34.53	84	FIES-prg 51-018
HIP79120	HR6011	16:08:58.87875	+03:27:16.1049	5.93	15.27	79	FIES-prg 51-018
HIP79219	HD145457	16:10:03.91431	+26:44:33.8927	6.57	-3.22	129	FIES-prg 51-018
HIP79488	9Her	16:13:15.42979	+05:01:15.9201	5.47	-1.15	99	FIES-prg 51-018
HIP79581	HR6057	16:14:13.60701	+05:54:06.6524	6.29	-21.66	106	FIES-prg 51-018
HIP79666	16Her	16:15:28.63502	+18:48:29.1149	5.69	-19.32	105	FIES-prg 51-018
HIP79953	HR6090	16:19:11.21370	+49:02:17.3767	5.91	-32.44	107	FIES-prg 51-018
HIP80514	HR6121	16:26:11.38549	+11:24:26.9793	6.11	-15.55	119	FIES-prg 51-018
HIP80693	HR6136	16:28:33.98107	+00:39:54.0122	5.39	8.11	79	FIES-prg 51-018
HIP80708	HD148531	16:28:42.31634	+00:03:17.4857	6.45	-8.48	73	FIES-prg 51-018
HIP81119	HD149474	16:34:04.24487	+25:28:36.2045	7.77	-9.48	97	FIES-prg 51-018
HIP82012	HR6230	16:45:11.79515	+43:13:01.8161	6.07	-12.96	108	FIES-prg 51-018
HIP82426	HR6259	16:50:43.15007	+32:33:13.1989	6.17	-23.24	126	FIES-prg 51-018
HIP82504	51Her	16:51:45.26230	+24:39:23.1581	5.04	-18.41	107	FIES-prg 51-018
HIP82611	HD152812	16:53:17.55584	+47:25:00.2104	5.99	-69.05	124	FIES-prg 51-018
HIP82764	HR6287	16:54:55.17042	+20:57:30.5626	5.40	-1.89	139	FIES-prg 51-018
HIP82802	54Her	16:55:22.16830	+18:25:59.5714	5.37	11.47	96	FIES-prg 51-018
HIP83347	HD154049	17:02:02.16642	+25:02:16.4735	7.79	-88.98	103	FIES-prg 51-018
HIP83504	HD154278	17:03:58.04241	+13:34:02.7035	6.06	46.25	118	FIES-prg 51-018
HIP83677	HR6358	17:06:09.64557	+09:44:01.9090	6.39	-6.49	100	FIES-prg 51-018
HIP83692	HR6364	17:06:18.04768	+22:05:02.9558	5.58	-96.50	98	FIES-prg 51-018
HIP84431	HR6419	17:15:41.47039	+23:44:33.9387	5.99	-43.84	99	FIES-prg 51-018
HIP84659	HD156774	17:18:24.52212	+26:56:12.8359	7.50	-52.18	108	FIES-prg 51-018
HIP84691	HR6443	17:18:48.52745	+28:49:22.6878	5.69	-12.20	117	FIES-prg 51-018
HIP84850	HD157326	17:20:30.17389	+44:11:31.6512	6.84	-33.57	114	FIES-prg 51-018
HIP84950	HR6479	17:21:45.36844	+53:25:13.5445	5.70	-7.25	107	FIES-prg 51-018
HIP85108	HD158147	17:23:37.70141	+60:59:54.7675	7.15	1.40	99	FIES-prg 53-002
HIP85109	HD157606	17:23:37.92491	+13:23:51.0513	7.48	0.75	87	FIES-prg 51-018
HIP85651	HD158823	17:30:14.61578	+29:30:26.9362	7.95	-49.65	113	FIES-prg 51-018
HIP85692	HR6540	17:30:43.57490	+57:52:36.5639	6.21	-12.72	110	FIES-prg 51-018
HIP85732	HD159027	17:31:11.52573	+28:08:10.8607	7.99	16.99	116	FIES-prg 51-018
HIP85766	HD158855	17:31:30.82839	+01:40:20.2780	7.18	-6.56	92	FIES-prg 51-018
HIP85824	HD159410	17:32:13.59053	+46:19:49.6314	7.29	-53.64	105	FIES-prg 51-018
HIP85838	HD159119	17:32:24.03475	+14:23:01.6837	7.01	-8.53	74	FIES-prg 51-018
HIP85888	HR6550	17:33:07.25794	+41:14:36.4179	5.73	-29.74	125	PolarBase
HIP86182	yHer	17:36:37.65447	+48:35:08.2751	5.36	26.62	126	FIES-prg 51-018
HIP86575	HR6590	17:41:32.32319	+06:18:47.3683	5.96	-30.08	122	FIES-prg 51-018
HIP86667	83Her	17:42:28.36218	+24:33:50.6133	5.57	-28.42	88	FIES-prg 51-018
HIP87194	87Her	17:48:49.14641	+25:37:22.3298	5.10	-25.09	108	FIES-prg 51-018
HIP87224	HR6639	17:49:19.04192	+01:57:41.0831	6.46	-59.88	103	FIES-prg 51-018
HIP87308	HR6654	17:50:22.89280	+29:19:19.7197	5.53	-15.24	115	FIES-prg 51-018

Table 4. Continued.

HIP/KIC/TYC	Alternative name	RA (J2000) (h:m:s)	Dec (J2000) (d:am:as)	V	v_{rad} km/s	S/N	Source
HIP87445	HR6673	17:52:04.72009	+39:58:55.5283	6.02	-69.60	109	FIES-prg 51-018
HIP87563	fHer	17:53:18.02749	+40:00:28.6595	5.18	-35.63	122	FIES-prg 51-018
HIP87585	ksiDra	17:53:31.72962	+56:52:21.5143	3.75	-25.83	106	FIES-prg 51-018
HIP87777	HR6687	17:55:50.81094	+22:27:51.1896	5.62	-44.12	101	FIES-prg 51-018
HIP88103	HD164575	17:59:36.87943	+43:14:07.3524	6.72	-10.87	113	FIES-prg 51-018
HIP88636	HR6768	18:05:49.61078	+32:13:50.4243	5.72	-0.06	91	PolarBase
HIP88701	HD165574	18:06:28.73410	+02:40:37.4680	8.88	-75.38	106	FIES-prg 51-018
HIP88770	HD165742	18:07:20.98434	+02:28:54.0172	6.49	-22.40	105	FIES-prg 51-018
HIP88877	HD166780	18:08:38.84546	+57:58:46.8655	7.34	-42.67	101	FIES-prg 51-018
HIP89065	HR6800	18:10:40.29954	+03:19:27.3253	5.50	6.18	113	FIES-prg 51-018
HIP89298	HR6820	18:13:16.56705	+21:52:49.2028	6.15	-90.12	105	FIES-prg 51-018
HIP89313	HD167275	18:13:26.91567	+26:14:38.4780	7.27	-5.25	126	FIES-prg 51-018
HIP89772	HD168387	18:19:09.53675	+07:15:35.1569	5.42	-8.40	115	FIES-prg 51-018
HIP89827	HR6867	18:19:52.06991	+29:39:59.0095	6.01	-38.20	105	FIES-prg 51-018
HIP89962	etaSer	18:21:18.60056	-02:53:55.7766	3.25	9.59	170	FIES-archive
HIP90067	HR6885	18:22:49.04004	+17:49:35.8121	5.26	-19.18	112	FIES-prg 51-018
HIP90069	HD169113	18:22:49.06958	+07:12:24.2911	7.08	-33.10	104	FIES-prg 51-018
HIP90344	42Dra	18:25:59.13734	+65:33:48.5288	4.83	32.36	148	FIES-archive
HIP90882	HD171992	18:32:18.79232	+67:46:36.7181	6.65	-20.75	96	FIES-prg 53-002
HIP90915	HR6966	18:32:46.15489	+23:37:00.4740	5.84	-7.35	106	FIES-prg 51-018
HIP91013	HR6983	18:33:56.69453	+52:21:12.6567	5.38	-24.11	113	FIES-prg 51-018
HIP91042	HD171550	18:34:19.72189	+29:44:30.3650	6.64	-17.35	120	FIES-prg 51-018
HIP91655	HD172651	18:41:26.68081	+00:33:51.8773	7.48	13.34	95	FIES-prg 51-018
HIP92088	HR7064	18:46:04.47990	+26:39:43.6641	4.84	-16.89	107	FIES-prg 51-018
HIP92731	HR7153	18:53:46.30964	+57:29:11.6082	6.24	-6.45	102	FIES-prg 53-002
HIP92768	HR7132	18:54:13.24771	+27:54:34.2964	5.62	14.28	102	FIES-prg 51-018
HIP92831	HD175740	18:54:52.17729	+41:36:09.7983	5.44	-9.35	117	FIES-prg 51-018
HIP92885	HD175955	18:55:33.32667	+47:26:26.7911	7.02	-22.67	99	FIES-prg 51-018
HIP92997	48Dra	18:56:45.05159	+57:48:53.4652	5.68	-39.31	97	FIES-prg 51-018
HIP93256	HR7181	18:59:45.48446	+26:13:49.4527	5.27	-22.62	120	FIES-prg 51-018
HIP93488	HR7208	19:02:21.56649	+08:22:24.7293	6.30	-11.78	109	FIES-prg 51-018
HIP93523	HR7216	19:02:52.62166	+19:39:39.6448	6.11	-7.49	110	FIES-prg 51-018
HIP93853	HD178612	19:06:51.49896	+48:55:31.7546	7.21	-4.51	104	FIES-prg 51-018
HIP93864	tauSgr	19:06:56.40897	-27:40:13.5189	3.31	40.59	128	FIES-prg 53-002
HIP94376	delDra	19:12:33.30197	+67:39:41.5456	3.07	24.87	173	FIES-prg 51-018
HIP94490	54Dra	19:13:55.14520	+57:42:18.3602	5.01	-32.31	101	FIES-prg 51-018
HIP94591	HD180315	19:14:58.47004	+28:23:40.7618	7.78	3.04	105	FIES-prg 51-018
HIP95291	HD182293	19:23:12.21573	+20:16:40.6007	7.11	-105.00	100	FIES-prg 51-018
HIP95480	HD182896	19:25:18.14891	+37:14:42.7121	6.80	-17.29	109	FIES-prg 51-018
HIP95498	4Vul	19:25:28.60332	+19:47:54.1214	5.16	0.98	124	FIES-prg 51-018
HIP96014	HR7427	19:31:19.33068	+50:18:24.1375	5.55	-9.90	123	FIES-prg 51-018
HIP96063	HD184150	19:31:55.99798	+30:11:16.4056	7.50	-34.10	93	FIES-prg 51-018
HIP96225	HD184538	19:34:02.26800	+25:48:21.0885	7.37	-24.41	110	FIES-prg 51-018
HIP96297	HD185394	19:34:46.35163	+63:26:03.0249	6.46	7.37	97	FIES-prg 53-002
HIP96449	HD185286	19:36:32.41897	+43:42:22.0049	6.57	-1.31	89	FIES-prg 53-002
HIP96457	HD185396	19:36:37.56017	+48:30:58.6035	6.99	-7.58	92	FIES-prg 53-002
HIP97789	HR7583	19:52:16.41396	+36:25:56.2635	6.10	-23.60	97	FIES-prg 51-018
HIP97859	HD188105	19:53:11.06507	+08:03:44.8066	7.61	-50.49	100	FIES-prg 51-018
HIP98110	etaCyg	19:56:18.37222	+35:05:00.3228	3.88	-26.14	126	FIES-prg 51-018
HIP98385	HR7636	19:59:22.64384	+01:22:39.7063	6.18	5.40	134	FIES-prg 51-018
HIP99291	HD192274	20:09:20.56155	+68:35:58.3921	6.97	-38.02	93	FIES-prg 53-002
HIP99623	HD192168	20:13:03.13659	+11:51:03.0694	6.51	10.91	96	FIES-prg 53-002
HIP99663	HR7742	20:13:27.61643	+60:38:26.0514	5.82	-4.03	101	FIES-prg 53-002
HIP101226	HD195647	20:31:06.89947	+40:51:28.8568	7.43	-22.62	99	PolarBase
HIP101245	HR7854	20:31:21.15124	+52:18:34.2918	6.22	-10.38	116	FIES-prg 53-002
HIP101899	HR7904	20:38:59.51695	+30:20:03.3579	5.69	11.68	115	FIES-prg 53-002
HIP101936	1Aqr	20:39:24.89096	+00:29:11.1909	5.15	-39.41	159	FIES-archive
HIP101979	HD196912	20:39:59.84331	+08:26:49.2611	6.84	0.40	106	FIES-prg 53-002
HIP101986	HR7919	20:40:03.15977	+43:27:31.9620	5.98	-23.82	114	FIES-prg 53-002
HIP101998	HD196870	20:40:12.51718	-02:39:18.3857	6.61	32.97	114	FIES-prg 53-002

Table 4. Continued.

HIP/KIC/TYC	Alternative name	RA (J2000) (h:m:s)	Dec (J2000) (d:am:as)	<i>V</i>	v_{rad} km/s	S/N	Source
HIP102080	10Del	20:41:16.20863	+14:34:58.3632	6.01	-24.74	104	FIES-prg 53-002
HIP102488	epsCyg	20:46:12.68236	+33:58:12.9250	2.48	-14.99	141	FIES-prg 51-018
HIP103598	HR8049	20:59:25.38477	+59:26:18.9341	5.54	-14.97	115	FIES-prg 53-002
HIP105411	34Vul	21:21:04.39426	+23:51:21.4872	5.57	-88.27	192	FIES-archive
HIP105502	1Peg	21:24:23.68430	+20:01:13.0015	4.09	-76.28	179	FIES-archive
HIP106081	HD204642	21:29:15.38603	+28:34:58.7948	6.76	20.16	151	FIES-archive
HIP106551	72Cyg	21:34:46.56384	+38:32:02.6049	4.91	-68.07	50	Thygesen et al. (2012)
HIP107119	11Cep	21:41:55.29337	+71:18:41.1062	4.54	-38.65	98	FIES-prg 53-002
HIP111944	11Lac	22:40:30.85881	+44:16:34.7042	4.46	-10.13	174	FIES-archive
HIP112041	HD215030	22:41:36.05160	+41:32:56.8433	5.92	-13.30	215	FIES-archive
HIP112067	HR8642	22:41:57.45572	+14:30:59.0145	5.93	-27.91	196	FIES-archive
HIP114200	4And	23:07:39.26716	+46:23:14.0225	5.31	-11.38	64	PolarBase
HIP114855	psi01Aqr	23:15:53.49482	-09:05:15.8546	4.25	-25.67	165	FIES-archive
HIP114971	gamPsc	23:17:09.93749	+03:16:56.2380	3.70	-14.63	254	PolarBase
HIP115830	tetPsc	23:27:58.09529	+06:22:44.3720	4.30	6.49	148	FIES-archive
HIP116823	HD222455	23:40:40.23712	+00:24:57.5144	7.44	-3.10	111	FIES-archive
KIC2425631	19081771+3745467	19:08:17.714	+37:45:46.73	11.03	18.63	37	Thygesen et al. (2012)
KIC2714397	19265491+3756300	19:26:54.914	+37:56:30.05	10.51	-172.24	40	Thygesen et al. (2012)
KIC3443331	19252667+3834356	19:25:26.676	+38:34:35.62	8.76	16.62	90	FIES-prg 51-018
KIC3748585	19272877+3848096	19:27:28.778	+38:48:09.65	8.60	-3.94	99	Thygesen et al. (2012)
KIC3748691	19273465+3850493	19:27:34.658	+38:50:49.34	11.59	3.84	36	Thygesen et al. (2012)
KIC3850749	19262003+3855272	19:26:20.035	+38:55:27.30	8.30	-2.80	94	FIES-prg 51-018
KIC3860139	19355873+3857327	19:35:58.733	+38:57:32.80	11.01	-6.12	30	Thygesen et al. (2012)
KIC3936921	19023934+3905592	19:02:39.348	+39:05:59.21	10.72	-35.77	34	Thygesen et al. (2012)
KIC3955590	19272677+3900456	19:27:26.777	+39:00:45.61	10.34	-52.56	37	Thygesen et al. (2012)
KIC4135680	18582100+3917443	18:58:21.000	+39:17:44.38	8.03	-19.27	106	FIES-prg 51-018
KIC4157282	19261103+3913424	19:26:11.033	+39:13:42.42	10.52	-20.49	32	Thygesen et al. (2012)
KIC4177025	19434309+3917436	19:43:43.097	+39:17:43.62	10.29	-102.45	36	Thygesen et al. (2012)
KIC4262505	19263055+3919247	19:26:30.557	+39:19:24.71	10.36	-9.82	54	Thygesen et al. (2012)
KIC4480358	19424053+3935234	19:42:40.536	+39:35:23.46	11.63	-84.46	35	Thygesen et al. (2012)
KIC4545666	19052956+3936000	19:05:29.558	+39:36:00.04	8.39	14.18	99	FIES-prg 51-018
KIC4659706	19324055+3946338	19:32:40.557	+39:46:33.85	9.94	-16.05	32	Thygesen et al. (2012)
KIC5113061	19413439+4017482	19:41:34.401	+40:17:48.30	11.16	2.92	33	Thygesen et al. (2012)
KIC5113910	19421943+4016074	19:42:19.433	+40:16:07.43	10.78	-5.98	38	Thygesen et al. (2012)
KIC5284127	19373122+4027511	19:37:31.221	+40:27:51.12	11.81	-67.26	29	Thygesen et al. (2012)
KIC5438922	19151849+4040055	19:15:18.490	+40:40:05.52	8.51	-21.48	99	FIES-prg 51-018
KIC5442047	19191870+4036083	19:19:18.703	+40:36:08.39	8.66	-56.85	99	FIES-prg 51-018
KIC5524720	19160889+4044237	19:16:08.890	+40:44:23.75	11.59	-35.14	26	Thygesen et al. (2012)
KIC5612549	19180824+4051167	19:18:08.247	+40:51:16.78	10.28	-2.81	61	Thygesen et al. (2012)
KIC5709564	19321853+4058217	19:32:18.535	+40:58:21.72	9.73	-86.35	52	Thygesen et al. (2012)
KIC5779724	19123427+4105257	19:12:34.279	+41:05:25.69	10.58	-53.59	53	Thygesen et al. (2012)
KIC5859492	19021718+4107236	19:02:17.189	+41:07:23.63	10.27	-63.37	42	Thygesen et al. (2012)
KIC5866965	19150476+4109509	19:15:04.759	+41:09:50.90	11.77	-65.82	33	Thygesen et al. (2012)
KIC5880651	19324393+4109335	19:32:43.932	+41:09:33.55	8.79	-19.52	83	FIES-prg 51-018
KIC5900096	19515137+4106378	19:51:51.379	+41:06:37.80	8.35	-36.17	36	Thygesen et al. (2012)
KIC6125893	19301223+4128369	19:30:12.228	+41:28:36.91	11.62	-35.91	27	Thygesen et al. (2012)
KIC6465075	19512404+4149284	19:51:24.045	+41:49:28.49	10.05	2.36	52	Thygesen et al. (2012)
KIC6515613	19184854+4155277	19:18:48.545	+41:55:27.70	8.17	-69.83	122	FIES-prg 51-018
KIC6547007	19525719+4158129	19:52:57.197	+41:58:12.94	10.42	-87.21	52	Thygesen et al. (2012)
KIC6606652	19275675+4200292	19:27:56.750	+42:00:29.23	8.53	-23.64	100	FIES-prg 51-018
KIC6676993	19080937+4206461	19:08:09.381	+42:06:46.19	8.78	-9.01	92	FIES-prg 51-018
KIC6680734	19135163+4211223	19:13:51.636	+42:11:22.31	11.68	13.02	38	Thygesen et al. (2012)
KIC6696436	19330045+4210000	19:33:00.454	+42:10:00.05	9.40	-8.16	60	Thygesen et al. (2012)
KIC6784681	19354484+4215280	19:35:44.847	+42:15:28.08	8.17	-46.14	106	FIES-prg 51-018
KIC6837256	18464309+4223144	18:46:43.090	+42:23:14.46	11.02	-6.79	50	Thygesen et al. (2012)
KIC7006979	18433894+4235295	18:43:38.947	+42:35:29.54	9.78	-47.99	60	Thygesen et al. (2012)
KIC7729396	18412961+4328163	18:41:29.616	+43:28:16.36	8.79	13.34	111	FIES-prg 51-018
KIC7889528	19251059+4339338	19:25:10.593	+43:39:33.84	8.25	7.11	91	FIES-prg 51-018
KIC7950369	19123111+4344145	19:12:31.114	+43:44:14.57	7.99	15.68	103	FIES-prg 51-018
KIC8005874	18435017+4350482	18:43:50.174	+43:50:48.19	8.36	-54.94	101	FIES-prg 51-018

Table 4. Continued.

HIP/KIC/TYC	Alternative name	RA (J2000) (h:m:s)	Dec (J2000) (d:am:as)	V	v_{rad} km/s	S/N	Source
KIC8167380	19294035+4403227	19:29:40.358	+44:03:22.79	8.30	-8.37	107	FIES-prg 51-018
KIC8172497	19363612+4401088	19:36:36.130	+44:01:08.80	8.64	-21.94	123	FIES-prg 51-018
KIC8617950	19165349+4446332	19:16:53.498	+44:46:33.20	8.19	-27.64	99	FIES-prg 51-018
KIC8873797	19073875+4509053	19:07:38.755	+45:09:05.36	11.91	-29.74	31	Thygesen et al. (2012)
KIC9205436	19014146+4536164	19:01:41.470	+45:36:16.42	8.22	-27.93	116	FIES-prg 51-018
KIC9326304	18542051+4549067	18:54:20.515	+45:49:06.74	8.46	-72.45	111	FIES-prg 51-018
KIC9474021	19411424+4601483	19:41:14.244	+46:01:48.36	10.91	-121.03	37	Thygesen et al. (2012)
KIC9529652	19324161+4606302	19:32:41.611	+46:06:30.20	8.74	-116.33	108	FIES-prg 51-018
KIC9665729	19511219+4618121	19:51:12.190	+46:18:12.17	8.83	7.59	83	FIES-prg 51-018
KIC9835672	19351093+4639586	19:35:10.932	+46:39:58.64	8.69	-35.73	95	FIES-prg 51-018
KIC9969701	19540112+4648501	19:54:01.119	+46:48:50.18	8.16	5.35	98	FIES-prg 51-018
KIC10186608	18444919+4717434	18:44:49.188	+47:17:43.48	11.14	-16.74	41	Thygesen et al. (2012)
KIC10190244	18533922+4713055	18:53:39.228	+47:13:05.52	7.97	-40.73	132	FIES-prg 51-018
KIC10403036	19243363+4732107	19:24:33.636	+47:32:10.75	10.80	-110.31	42	Thygesen et al. (2012)
KIC10649021	18550791+4754062	18:55:07.918	+47:54:06.23	10.98	-40.39	33	Thygesen et al. (2012)
KIC10802990	19363245+4811584	19:36:32.458	+48:11:58.45	8.50	-2.38	108	FIES-prg 51-018
KIC11045542	19530590+4833180	19:53:05.906	+48:33:18.04	10.95	23.43	45	Thygesen et al. (2012)
KIC11246393	19315785+4858462	19:31:57.859	+48:58:46.20	8.81	-16.33	106	FIES-prg 51-018
KIC11342694	19110062+4906529	19:11:00.622	+49:06:52.99	9.86	-8.47	43	Thygesen et al. (2012)
KIC11444313	19014380+4923062	19:01:43.810	+49:23:06.22	11.31	-18.55	42	Thygesen et al. (2012)
KIC11555150	19182462+4933536	19:18:24.619	+49:33:53.64	8.51	6.51	105	FIES-prg 51-018
KIC11569659	19464387+4934210	19:46:43.874	+49:34:21.00	11.51	-12.72	46	Thygesen et al. (2012)
KIC11657684	19175551+4946243	19:17:55.517	+49:46:24.38	11.71	17.44	34	Thygesen et al. (2012)
KIC12457780	19195017+5120078	19:19:50.172	+51:20:07.84	8.82	-25.00	101	FIES-prg 51-018
TYC324-266-1	14231899+0540079	14:23:18.996	+05:40:07.91	10.67	-123.93	95	FIES-prg 53-002
TYC336-147-1	15152288+0126456	15:15:22.8847	+01:26:45.548	9.96	5.14	112	FIES-prg 53-002
TYC1570-1460-1	18330861+1530299	18:33:08.5991	+15:30:30.034	9.83	1.50	123	FIES-prg 53-002
TYC2012-1102-1	14062451+2853085	14:06:24.5138	+28:53:08.336	9.97	31.81	106	FIES-prg 53-002
TYC2041-1586-1	16001507+2807036	16:00:15.0835	+28:07:03.865	9.99	-12.08	118	FIES-prg 53-002
TYC2046-759-1	16113361+2436523	16:11:33.608	+24:36:52.33	11.14	-14.07	83	FIES-prg 53-002
TYC3026-782-1	13385176+3850476	13:38:51.7653	+38:50:47.607	9.76	11.21	121	FIES-prg 53-002
TYC3041-648-1	14132200+4412525	14:13:21.9997	+44:12:52.477	9.94	-89.42	102	FIES-prg 53-002
TYC3044-14-1	14562434+3825064	14:56:24.3354	+38:25:06.501	9.75	-41.79	103	FIES-prg 53-002
TYC3051-805-1	15080646+4320586	15:08:06.4691	+43:20:58.532	9.83	0.33	107	FIES-prg 53-002
TYC3051-1340-1	15160507+4322192	15:16:05.0731	+43:22:19.323	9.72	-14.42	118	FIES-prg 53-002
TYC3054-1026-1	15492544+3816041	15:49:25.4467	+38:16:04.279	9.86	39.66	113	FIES-prg 53-002
TYC3058-519-1	15220070+4251531	15:22:00.7028	+42:51:53.124	9.82	23.22	117	FIES-prg 53-002
TYC3059-694-1	15343532+4331285	15:34:35.3321	+43:31:28.630	9.92	38.62	98	FIES-prg 53-002
TYC3064-391-1	16114810+4136200	16:11:48.0998	+41:36:20.006	9.92	-99.87	110	FIES-prg 53-002
TYC3064-897-1	16110090+4126011	16:11:00.9082	+41:26:01.283	9.62	-71.79	110	FIES-prg 53-002
TYC3071-1491-1	16570334+3912158	16:57:03.3437	+39:12:15.952	9.49	-120.49	126	FIES-prg 53-002
TYC3074-1109-1	16405592+3958217	16:40:55.9296	+39:58:21.747	9.58	-9.29	119	FIES-prg 53-002
TYC3094-1605-1	17215666+4301408	17:21:56.6837	+43:01:40.687	10.40	-81.05	112	FIES-prg 53-002
TYC3132-453-1	19084773+4342435	19:08:47.7325	+43:42:43.524	9.85	32.16	123	FIES-prg 53-002
TYC3465-458-1	14103640+4547187	14:10:36.4018	+45:47:18.765	9.64	-15.28	105	FIES-prg 53-002
TYC3494-279-1	16064753+4921349	16:06:47.5608	+49:21:35.001	9.92	-69.90	118	FIES-prg 53-002
TYC3494-461-1	16093875+4820265	16:09:38.7665	+48:20:26.693	9.50	-24.74	115	FIES-prg 53-002
TYC3495-780-1	16164332+4929538	16:16:43.3283	+49:29:53.684	9.66	-92.50	122	FIES-prg 53-002
TYC3500-405-1	16470722+4626037	16:47:07.2209	+46:26:03.617	9.83	-114.09	116	FIES-prg 53-002
TYC3504-1938-1	17115703+4802040	17:11:57.0424	+48:02:04.084	9.93	-9.32	110	FIES-prg 53-002
TYC3844-739-1	12320787+5727284	12:32:07.8711	+57:27:28.396	9.51	5.49	103	FIES-prg 53-002
TYC3859-503-1	14145589+5417365	14:14:55.8962	+54:17:36.579	10.81	-67.88	92	FIES-prg 53-002
TYC3870-557-1	15484261+5424001	15:48:42.6161	+54:24:00.085	9.47	6.70	120	FIES-prg 53-002

Table 5. Atomic data for the spectral lines used in the analysis. The first part list the lines used in the determination of the stellar parameters and calcium abundance, while the second part list the lines used to determine the oxygen, magnesium, and titanium abundances. All atomic data are collected by the Gaia-ESO line list group (Heiter et al. 2015b). For the three Ca I-lines marked with asterisks only the gravity-sensitive wings are used. The references are for wavelength, $\log gf$, and excitation energy respectively. In cases where several references are given for a quantity the value listed is a mean of the reference values.

Element	Wavelength (Å) (air)	$\log gf$	χ_{exc} (eV)	References
Fe I	5778.4533	-3.430	2.588	1, 2, 1
Fe I	5855.0758	-1.478	4.608	1, 2, 1
Fe I	6012.2098	-4.038	2.223	1, 3, 1
Fe I	6027.0508	-1.089	4.076	1, 4, 1
Fe I	6120.2464	-5.970	0.915	1, 5, 1
Fe I	6136.9938	-2.950	2.198	1, 4+6, 1
Fe I	6151.6173	-3.295	2.176	1, 3+4+6, 1
Fe I	6165.3598	-1.473	4.143	1, 4, 1
Fe I	6173.3343	-2.880	2.223	1, 6, 1
Fe I	6213.4294	-2.481	2.223	1, 4, 1
Fe I	6271.2779	-2.703	3.332	1, 2, 1
Fe I	6322.6850	-2.430	2.588	1, 4+7, 1
Fe I	6335.3299	-2.177	2.198	1, 4, 1
Fe I	6411.6480	-0.596	3.654	1, 3+4+8, 1
Fe I	6518.3657	-2.438	2.832	1, 2+4, 1
Fe I	6581.2092	-4.679	1.485	1, 3, 1
Fe I	6593.8695	-2.420	2.433	1, 4+6, 1
Fe I	6609.1097	-2.691	2.559	1, 4+7, 1
Fe I	6633.7487	-0.799	4.559	1, 4, 1
Fe I	6739.5204	-4.794	1.557	1, 3, 1
Fe I	6793.2582	-2.326	4.076	1, 2, 1
Fe I	6810.2622	-0.986	4.607	1, 4, 1
Fe I	6828.5912	-0.820	4.638	9, 10, 1
Fe I	6837.0056	-1.687	4.593	1, 2, 1
Fe I	6843.6554	-0.730	4.549	1, 11, 1
Fe II	5991.3721	-3.540	3.153	12, 13, 14
Fe II	6084.1030	-3.790	3.200	12, 13, 14
Fe II	6113.3192	-4.140	3.221	12, 13, 14
Fe II	6149.2459	-2.690	3.889	12, 13, 14
Fe II	6247.5590	-2.300	3.892	12, 13, 14
Fe II	6432.6772	-3.570	2.891	12, 13, 14
Fe II	6456.3805	-2.050	3.903	12, 13, 14
Ca I	5867.5620	-1.570	2.933	15, 15, 15
Ca I*	6122.2170	-0.380	1.886	16, 17, 16
Ca I*	6162.1730	-0.170	1.899	16, 17, 16
Ca I	6166.4390	-1.142	2.521	18+19, 18, 18+19
Ca I	6169.0420	-0.797	2.523	18+19, 18, 18+19
Ca I*	6439.0750	0.390	2.526	18+19, 18, 18+19
Ca I	6499.6500	-0.818	2.523	18+19, 18, 18+19
O I	6300.3038	-9.715	0.000	20, 21+22, 23
Mg I	6318.7170	-2.020	5.108	23, 24, 23
Mg I	6319.2370	-2.242	5.108	23, 24, 23
Mg I	6319.4930	-2.719	5.108	23, 24, 23
Ti I	6091.1710	-0.320	2.267	25, 26, 25
Ti I	6092.7918	-1.380	1.887	25, 26, 25
Ti I	6336.0993	-1.690	1.443	25, 26, 25
Ti I	6395.4718	-2.540	1.503	25, 26, 25

References.

(1) Kurucz (2007); (2) Bard & Kock (1994); (3) Bard et al. (1991); (4) O’Brian et al. (1991); (5) Blackwell et al. (1986); (6) Blackwell et al. (1982a); (7) Blackwell et al. (1982b); (8) Den Hartog et al. (2014); (9) Fuhr et al. (1988); (10) May et al. (1974); (11) Ruffoni et al. (2014); (12) Nave & Johansson (2013); (13) Meléndez & Barbuy (2009); (14) Kurucz (2013); (15) Smith (1988); (16) Smith & O’Neill (1975); (17) Aldenius et al. (2009); (18) Smith & Raggett (1981); (19) Smith (1981); (20) Wiese et al. (1966); (21) Storey & Zeippen (2000); (22) Froese Fischer & Tachiev (2012); (23) Ralchenko et al. (2010); (24) Pehlivan et al. (in prep); (25) Lawler et al. (2013a); (26) Lawler et al. (2013b)

Table 6. Determined stellar parameters and abundances for the observed giants. The reference values for T_{eff} are from Mozurkewich et al. (2003) and the reference values for $\log g$ are from Huber et al. (2014)

HIP/KIC/TYC	$T_{\text{eff,ref}}$	T_{eff}	$\log g_{\text{ref}}$	$\log g$	[Fe/H]	v_{mic}	A(O)	A(Mg)	A(Ca)	A(Ti)
HIP1692	...	4216	...	1.79	-0.29	1.55	...	7.50	6.10	4.68
HIP9884	4493 ± 55	4464	...	2.27	-0.24	1.34	8.57	7.47	6.16	4.72
HIP10085	...	4062	...	1.44	-0.35	1.63	...	7.37	6.03	4.60
HIP12247	...	4790	...	2.71	-0.07	1.40	8.69	7.53	6.33	4.83
HIP28417	...	4746	...	2.56	-0.28	1.40	8.63	7.44	6.16	4.67
HIP33827	...	4235	...	1.99	-0.02	1.50	...	7.65	6.34	4.87
HIP35759	...	4606	...	2.47	-0.18	1.42	8.74	7.63	6.25	4.80
HIP37447	...	4758	...	2.73	-0.07	1.35	8.68	7.55	6.28	4.78
HIP37826	4858 ± 60	4835	...	2.93	0.04	1.24	8.69	7.63	6.43	4.92
HIP43813	...	4873	...	2.62	-0.10	1.51	8.66	7.49	6.33	4.77
HIP46390	4060 ± 50	4095	...	1.56	-0.10	1.77	8.63	7.56	6.22	4.82
HIP48455	...	4461	...	2.65	0.20	1.55	8.93	7.83	6.50	5.13
HIP50583	...	4341	...	1.77	-0.48	1.56	8.43	7.26	5.93	4.47
HIP52943	...	4310	...	1.87	-0.27	1.55	8.55	7.49	6.11	4.67
HIP53740	...	4621	...	2.44	-0.11	1.42	8.66	7.57	6.28	4.77
HIP54539	4550 ± 56	4534	...	2.33	-0.10	1.46	8.64	7.42	6.28	4.79
HIP55219	4091 ± 50	4133	...	1.65	-0.17	1.72	8.73	7.33	6.15	4.70
HIP57477	...	4400	...	2.60	0.23	1.52	8.93	7.76	6.51	5.12
HIP58628	...	4525	...	2.21	-0.26	1.49	8.65	7.37	6.15	4.67
HIP63432	...	4195	...	1.21	-0.90	1.81	8.32	7.02	5.57	4.22
HIP64022	...	3916	...	1.28	-0.19	1.47	8.48	7.53	6.20	4.76
HIP65028	...	4768	...	2.64	-0.53	1.29	...	7.20	5.96	4.43
HIP66726	...	4546	...	2.57	-0.07	1.52	8.87	7.74	6.29	4.94
HIP66900	...	4684	...	2.80	-0.22	1.24	8.72	7.66	6.27	4.90
HIP67608	...	4496	...	1.97	-0.44	1.52	8.48	7.28	6.05	4.53
HIP68501	...	3925	...	1.32	-0.50	1.41	8.49	7.53	6.00	4.70
HIP68567	...	4190	...	1.95	-0.17	1.46	8.64	7.58	6.21	4.81
HIP68739	...	4258	...	2.52	0.15	1.38	8.86	7.84	6.49	5.13
HIP68763	...	4778	...	2.81	0.02	1.46	8.80	7.62	6.41	4.90
HIP68932	...	4827	...	2.70	-0.20	1.42	...	7.46	6.21	4.70
HIP68955	...	4806	...	2.69	-0.22	1.35	8.68	7.42	6.18	4.65
HIP69067	...	3928	...	1.27	-0.20	1.47	8.47	7.58	6.19	4.75
HIP69107	...	4744	...	2.53	-0.28	1.48	8.73	7.42	6.16	4.71
HIP69118	...	4152	...	1.86	-0.21	1.42	8.61	7.57	6.20	4.78
HIP69127	...	4799	...	2.76	-0.32	1.27	8.57	7.27	6.13	4.63
HIP69198	...	4490	...	2.63	0.09	1.41	...	7.74	6.42	5.03
HIP69253	...	4202	...	2.03	-0.15	1.47	8.66	7.55	6.19	4.81
HIP69295	...	4778	...	2.48	-0.37	1.39	...	7.44	6.11	4.59
HIP69316	...	4433	...	2.70	0.24	1.48	...	7.88	6.52	5.14
HIP69585	...	4174	...	1.98	-0.10	1.44	8.65	7.60	6.28	4.90
HIP69612	...	4716	...	2.56	-0.16	1.42	8.71	7.48	6.23	4.72
HIP69673	4226 ± 53	4251	...	1.72	-0.60	1.64	8.57	7.38	5.88	4.54
HIP70548	...	4238	...	2.33	-0.00	1.36	8.79	7.75	6.36	5.02
HIP70899	...	3921	...	1.48	0.05	1.37	...	7.66	6.42	5.08
HIP70949	...	4085	...	1.60	-0.30	1.52	8.54	7.45	6.09	4.65
HIP71568	...	3917	...	1.09	-0.91	1.61	8.29	7.13	5.60	4.27
HIP71996	...	4767	...	2.56	-0.41	1.51	8.70	7.47	6.11	4.68
HIP72012	...	4055	...	1.43	-0.43	1.51	8.43	7.41	6.00	4.57
HIP72462	...	4341	...	2.18	-0.33	1.39	...	7.66	6.17	4.82
HIP72499	...	4440	...	2.68	0.30	1.55	8.94	7.99	6.58	5.20
HIP72607	3849 ± 47	3992	...	1.32	-0.23	1.60	8.54	7.40	6.12	4.73
HIP72664	...	4131	...	1.79	-0.20	1.50	8.54	7.54	6.18	4.78
HIP73203	...	4044	...	1.49	-0.58	1.43	8.52	7.45	5.98	4.67
HIP73388	...	4780	...	2.45	-0.36	1.36	...	7.26	6.15	4.56
HIP73568	...	3933	...	1.26	-0.14	1.48	8.51	7.59	6.27	4.79
HIP73745	...	4316	...	1.95	-0.25	1.55	8.59	7.48	6.14	4.71
HIP73909	...	4866	...	2.56	-0.40	1.44	8.57	7.32	6.05	4.52
HIP73917	...	4216	...	1.96	-0.14	1.52	8.60	7.62	6.24	4.83
HIP73991	...	4887	...	2.47	-0.72	1.50	...	7.30	5.93	4.38
HIP74649	...	4468	...	2.33	-0.00	1.41	8.73	7.51	6.30	4.84

Table 6. Continued.

HIP/KIC/TYC	$T_{\text{eff,ref}}$	T_{eff}	$\log g_{\text{ref}}$	$\log g$	[Fe/H]	v_{mic}	A(O)	A(Mg)	A(Ca)	A(Ti)
HIP74666	4850 ± 60	4861	...	2.63	-0.37	1.42	...	7.35	6.11	4.62
HIP75119	...	4380	...	2.36	-0.08	1.32	8.64	7.62	6.32	4.89
HIP75127	...	4820	...	2.89	0.17	1.42	8.82	7.76	6.55	5.04
HIP75260	...	4278	...	2.37	0.04	1.45	8.84	7.74	6.35	5.02
HIP75369	...	4455	...	2.37	-0.01	1.46	...	7.61	6.35	4.87
HIP75541	...	4123	...	1.84	-0.07	1.50	...	7.57	6.27	4.83
HIP75572	...	4019	...	1.39	-0.45	1.48	8.42	7.39	6.00	4.60
HIP75583	...	4177	...	1.71	-0.42	1.50	8.54	7.38	5.97	4.57
HIP75822	...	4142	...	1.93	-0.01	1.50	8.71	7.65	6.32	4.86
HIP76333	...	4762	...	2.59	-0.37	1.32	8.52	7.33	6.08	4.58
HIP76634	...	4100	...	2.13	0.16	1.42	...	7.87	6.53	5.15
HIP77070	4558 ± 56	4540	...	2.61	0.16	1.43	8.86	7.82	6.48	5.07
HIP77578	...	4773	...	2.55	-0.24	1.40	8.58	7.47	6.22	4.68
HIP77743	...	4404	...	2.48	0.24	1.42	8.85	7.86	6.56	5.14
HIP77748	...	4412	...	2.44	-0.03	1.38	8.68	7.60	6.31	4.89
HIP78132	...	4523	...	2.69	-0.01	1.28	8.85	7.77	6.42	5.03
HIP78157	...	4439	...	2.67	0.24	1.58	8.93	7.92	6.52	5.15
HIP78262	...	4049	...	1.77	-0.03	1.46	8.65	7.62	6.33	4.92
HIP79120	...	4051	...	1.91	0.05	1.41	8.70	7.66	6.41	5.06
HIP79219	...	4745	...	2.50	-0.24	1.43	...	7.39	6.20	4.70
HIP79488	...	4030	...	1.54	-0.13	1.58	8.54	7.65	6.25	4.83
HIP79581	...	4500	...	2.59	-0.03	1.29	8.65	7.65	6.33	4.91
HIP79666	...	4629	...	2.63	0.10	1.38	8.75	7.70	6.44	4.96
HIP79953	...	4126	...	1.68	-0.20	1.49	8.59	7.45	6.17	4.73
HIP80514	...	4717	...	2.60	-0.13	1.43	8.65	7.50	6.26	4.77
HIP80693	...	4096	...	1.95	0.07	1.61	8.77	7.70	6.40	5.01
HIP80708	...	4253	...	2.49	0.17	1.46	...	7.84	6.51	5.18
HIP81119	...	3923	...	1.24	-0.26	1.48	...	7.52	6.12	4.69
HIP82012	...	4061	...	1.55	-0.25	1.49	8.54	7.55	6.15	4.72
HIP82426	...	4686	...	2.71	-0.23	1.19	8.65	7.45	6.20	4.68
HIP82504	...	4459	...	1.99	-0.11	1.81	8.63	7.41	6.24	4.73
HIP82611	...	4193	...	1.70	-0.48	1.54	8.53	7.30	5.93	4.54
HIP82764	...	4896	...	2.76	-0.17	1.36	...	7.48	6.27	4.75
HIP82802	...	4075	...	1.73	-0.16	1.45	8.61	7.52	6.26	4.87
HIP83347	...	4256	...	2.07	-0.15	1.46	...	7.54	6.27	4.85
HIP83504	...	4664	...	2.62	-0.29	1.30	8.55	7.33	6.15	4.70
HIP83677	...	4066	...	1.66	-0.12	1.52	8.60	7.60	6.25	4.80
HIP83692	...	4237	...	2.10	-0.08	1.40	8.79	7.71	6.31	4.88
HIP84431	...	4253	...	1.98	-0.06	1.58	8.68	7.60	6.25	4.83
HIP84659	...	4355	...	2.01	-0.19	1.55	...	7.41	6.16	4.70
HIP84691	...	4896	...	2.82	-0.09	1.37	8.69	7.48	6.34	4.80
HIP84850	...	4614	...	2.38	-0.12	1.40	8.64	7.42	6.27	4.76
HIP84950	...	3954	...	1.11	-0.27	1.53	8.42	7.44	6.14	4.61
HIP85108	...	4388	...	2.23	-0.14	1.41	...	7.53	6.27	4.84
HIP85109	...	4274	...	2.31	0.05	1.35	...	7.73	6.38	5.00
HIP85651	...	4215	...	1.76	-0.28	1.59	...	7.43	6.08	4.67
HIP85692	...	4107	...	1.59	-0.22	1.54	8.55	7.40	6.14	4.65
HIP85732	...	4355	...	1.98	-0.36	1.46	8.55	7.39	6.07	4.62
HIP85766	...	4438	...	2.48	0.05	1.41	8.75	7.69	6.40	4.95
HIP85824	...	4080	...	1.68	-0.36	1.37	...	7.60	6.16	4.82
HIP85838	...	3936	...	1.61	0.09	1.57	8.64	7.86	6.40	5.02
HIP85888	...	4553	...	2.34	-0.34	1.31	8.50	7.39	6.13	4.62
HIP86182	...	4510	...	2.24	-0.34	1.35	8.55	7.33	6.09	4.58
HIP86575	...	4511	...	2.02	-0.16	1.84	8.62	7.48	6.24	4.76
HIP86667	...	3966	...	1.59	-0.19	1.38	8.59	7.72	6.23	4.89
HIP87194	...	4526	...	2.55	-0.01	1.45	8.86	7.73	6.39	5.02
HIP87224	...	4527	...	2.56	0.04	1.45	8.81	7.68	6.36	4.94
HIP87308	...	4635	...	2.65	-0.13	1.27	8.64	7.49	6.26	4.77
HIP87445	...	4207	...	1.78	-0.26	1.53	8.58	7.44	6.14	4.69
HIP87563	...	4448	...	2.37	-0.10	1.49	8.74	7.56	6.28	4.84
HIP87585	...	4472	...	2.56	0.01	1.30	8.75	7.63	6.37	4.95

Table 6. Continued.

HIP/KIC/TYC	$T_{\text{eff,ref}}$	T_{eff}	$\log g_{\text{ref}}$	$\log g$	[Fe/H]	v_{mic}	A(O)	A(Mg)	A(Ca)	A(Ti)
HIP87777	...	4387	...	2.21	-0.02	1.49	...	7.56	6.32	4.86
HIP88103	...	4535	...	2.63	-0.13	1.25	8.53	7.59	6.25	4.81
HIP88636	...	4537	...	2.21	-0.09	1.54	8.67	7.48	6.30	4.78
HIP88701	...	4338	...	2.08	-0.21	1.44	...	7.48	6.20	4.75
HIP88770	...	4066	...	1.64	-0.25	1.50	8.56	7.46	6.13	4.73
HIP88877	...	4012	...	1.46	-0.27	1.46	...	7.52	6.14	4.72
HIP89065	...	4511	...	2.42	-0.00	1.47	...	7.61	6.35	4.89
HIP89298	...	4012	...	1.34	-0.36	1.49	8.44	7.43	6.06	4.59
HIP89313	...	4484	...	2.16	-0.48	1.44	8.47	7.24	5.95	4.52
HIP89772	...	4555	...	2.83	-0.10	1.17	8.70	7.74	6.32	4.94
HIP89827	...	4286	...	2.06	-0.10	1.59	...	7.55	6.22	4.79
HIP89962	...	4849	...	2.96	-0.29	1.15	8.51	7.43	6.18	4.66
HIP90067	...	4366	...	2.14	-0.16	1.44	8.67	7.49	6.22	4.78
HIP90069	...	4411	...	2.05	-0.15	1.68	8.59	7.48	6.20	4.73
HIP90344	...	4359	...	1.86	-0.52	1.44	8.34	7.34	5.95	4.52
HIP90882	...	4091	...	1.55	-0.15	1.57	8.58	7.44	6.25	4.73
HIP90915	...	4018	...	1.40	-0.18	1.61	8.54	7.43	6.17	4.69
HIP91013	...	4726	...	2.31	-0.12	1.68	8.66	7.49	6.31	4.79
HIP91042	...	4739	...	2.47	-0.28	1.42	8.63	7.46	6.15	4.68
HIP91655	...	4163	...	1.96	-0.04	1.50	...	7.64	6.29	4.88
HIP92088	...	4426	...	2.34	-0.07	1.33	8.70	7.56	6.30	4.84
HIP92731	...	4352	...	2.17	-0.10	1.44	8.59	7.55	6.27	4.80
HIP92768	...	4147	...	1.84	-0.19	1.42	...	7.55	6.20	4.81
HIP92831	...	4788	...	2.82	0.03	1.33	8.72	7.60	6.42	4.91
HIP92885	...	4483	...	2.63	-0.03	1.29	8.71	7.65	6.33	4.88
HIP92997	...	4519	...	2.63	0.01	1.34	...	7.71	6.36	4.94
HIP93256	...	4331	...	2.09	-0.28	1.39	8.58	7.42	6.12	4.71
HIP93488	...	4129	...	1.61	-0.18	1.75	8.64	7.39	6.16	4.72
HIP93523	...	4445	...	2.13	-0.09	1.72	8.70	7.48	6.24	4.78
HIP93853	...	4157	...	1.74	-0.17	1.59	8.60	7.52	6.19	4.75
HIP93864	...	4434	...	2.25	-0.22	1.39	8.61	7.47	6.17	4.70
HIP94376	4851 ± 67	4807	...	2.71	-0.17	1.35	8.66	7.40	6.24	4.72
HIP94490	...	4513	...	2.67	-0.00	1.31	8.75	7.73	6.36	4.91
HIP94591	...	4216	...	1.83	-0.18	1.57	8.64	7.48	6.16	4.73
HIP95291	...	4490	...	2.77	-0.01	1.21	8.74	7.84	6.42	5.06
HIP95480	...	4506	...	2.63	-0.12	1.16	8.70	7.65	6.33	4.92
HIP95498	...	4819	...	2.67	-0.13	1.38	8.60	7.49	6.31	4.78
HIP96014	...	4291	...	1.78	-0.40	1.61	8.45	7.32	5.96	4.55
HIP96063	...	4215	...	2.10	-0.07	1.46	...	7.62	6.27	4.87
HIP96225	...	4355	...	2.07	-0.11	1.51	8.69	7.48	6.25	4.75
HIP96297	...	4224	...	1.98	-0.15	1.44	...	7.54	6.23	4.82
HIP96449	...	4045	...	1.67	-0.10	1.58	8.63	7.60	6.22	4.84
HIP96457	...	4004	...	1.63	-0.12	1.55	8.52	7.54	6.22	4.80
HIP97789	...	4110	...	1.73	-0.05	1.60	8.69	7.56	6.28	4.84
HIP97859	...	4582	...	2.54	-0.02	1.45	8.68	7.63	6.32	4.85
HIP98110	...	4788	...	2.76	0.01	1.38	8.69	7.59	6.42	4.87
HIP98385	...	4600	...	2.04	-0.62	1.58	8.38	7.11	5.84	4.37
HIP99291	...	4315	...	2.19	-0.01	1.51	...	7.60	6.34	4.90
HIP99623	...	4465	...	2.53	-0.00	1.36	8.72	7.60	6.34	4.90
HIP99663	...	3949	...	1.39	-0.26	1.51	8.47	7.46	6.13	4.70
HIP101226	...	4819	...	2.69	-0.18	1.34	8.62	7.45	6.27	4.72
HIP101245	...	4758	...	2.73	-0.15	1.25	8.53	7.44	6.27	4.72
HIP101899	...	4637	...	2.46	-0.15	1.44	8.69	7.53	6.26	4.76
HIP101936	...	4750	...	2.75	0.05	1.41	8.79	7.59	6.41	4.91
HIP101979	...	4744	...	2.78	0.03	1.43	8.81	7.65	6.39	4.93
HIP101986	...	4449	...	2.27	-0.27	1.41	8.65	7.35	6.12	4.68
HIP101998	...	4735	...	2.67	-0.10	1.36	8.78	7.50	6.30	4.79
HIP102080	...	4378	...	2.27	-0.03	1.40	...	7.58	6.32	4.87
HIP102488	4756 ± 59	4711	...	2.59	-0.18	1.35	8.66	7.50	6.23	4.74
HIP103598	...	4068	...	1.41	-0.41	1.66	...	7.31	5.97	4.54
HIP105411	...	4623	...	2.44	-0.27	1.44	...	7.64	6.20	4.78

Table 6. Continued.

HIP/KIC/TYC	$T_{\text{eff,ref}}$	T_{eff}	$\log g_{\text{ref}}$	$\log g$	[Fe/H]	v_{mic}	A(O)	A(Mg)	A(Ca)	A(Ti)
HIP105502	...	4612	...	2.56	-0.04	1.43	8.76	7.63	6.34	4.87
HIP106081	...	4616	...	2.88	-0.01	1.22	8.71	7.63	6.36	4.91
HIP106551	...	4624	...	2.51	-0.06	1.44	8.68	7.56	6.29	4.78
HIP107119	...	4664	...	2.78	0.16	1.41	...	7.70	6.48	5.00
HIP111944	...	4283	...	1.96	-0.18	1.51	8.65	7.44	6.16	4.70
HIP112041	...	4745	...	2.64	-0.47	1.27	8.46	7.26	5.99	4.50
HIP112067	...	4656	...	2.67	-0.05	1.56	8.68	7.64	6.34	4.92
HIP114200	...	4118	...	1.97	0.01	1.51	8.73	7.70	6.36	4.98
HIP114855	...	4610	...	2.53	-0.03	1.41	8.74	7.61	6.31	4.86
HIP114971	...	4870	...	2.53	-0.59	1.47	8.60	7.34	6.00	4.53
HIP115830	...	4704	...	2.72	0.05	1.41	8.83	7.63	6.39	4.92
HIP116823	...	4474	...	2.81	0.06	1.27	8.84	7.79	6.42	5.05
KIC2425631	...	4482	2.250 ± 0.025	2.23	-0.28	1.43	8.59	7.47	6.18	4.70
KIC2714397	...	4870	2.450 ± 0.028	2.63	-0.56	1.47	8.78	7.44	6.08	4.64
KIC3443331	...	4293	...	2.18	0.08	1.58	8.81	7.67	6.42	5.01
KIC3748585	...	4542	2.583 ± 0.023	2.64	0.01	1.26	8.71	7.65	6.37	4.93
KIC3748691	...	4695	2.506 ± 0.027	2.68	-0.05	1.44	...	7.60	6.32	4.85
KIC3850749	...	4058	...	1.49	-0.13	1.57	8.56	7.50	6.23	4.75
KIC3860139	...	4392	2.223 ± 0.031	2.34	-0.01	1.37	8.82	7.68	6.31	4.82
KIC3936921	...	4397	2.357 ± 0.029	2.25	-0.04	1.43	8.66	7.76	6.32	4.87
KIC3955590	...	4415	2.225 ± 0.026	2.45	-0.00	1.57	...	7.65	6.33	4.93
KIC4135680	...	4202	...	1.84	-0.18	1.39	8.60	7.52	6.23	4.78
KIC4157282	...	4397	2.089 ± 0.029	2.15	-0.19	1.40	8.64	7.51	6.28	4.76
KIC4177025	...	4254	1.660 ± 0.029	1.67	-0.53	1.55	8.64	7.56	6.02	4.65
KIC4262505	...	4829	2.880 ± 0.028	2.89	-0.25	1.19	8.57	7.43	6.18	4.71
KIC4480358	...	4534	1.849 ± 0.031	2.27	-0.83	1.41	...	7.06	5.66	4.30
KIC4545666	...	4293	...	2.17	-0.06	1.44	8.70	7.66	6.29	4.86
KIC4659706	...	4367	2.458 ± 0.029	2.49	0.20	1.40	8.87	7.85	6.56	5.12
KIC5113061	...	4084	1.536 ± 0.026	1.77	-0.07	1.63	...	7.57	6.25	4.85
KIC5113910	...	4371	1.750 ± 0.026	1.79	-0.46	1.56	8.44	7.27	5.98	4.47
KIC5284127	...	4501	2.459 ± 0.029	2.50	0.09	1.53	8.79	7.78	6.43	5.02
KIC5438922	...	4107	...	1.78	-0.15	1.53	8.74	7.70	6.25	4.91
KIC5442047	...	4079	...	1.69	-0.13	1.50	8.60	7.52	6.25	4.79
KIC5524720	...	4243	2.229 ± 0.029	2.27	0.08	1.32	8.72	7.66	6.37	4.95
KIC5612549	...	4833	2.385 ± 0.030	2.65	-0.41	1.44	...	7.29	6.00	4.53
KIC5709564	...	4689	2.373 ± 0.029	2.50	-0.39	1.56	...	7.62	6.18	4.78
KIC5779724	...	4258	1.678 ± 0.028	1.81	-0.50	1.57	...	7.40	6.03	4.66
KIC5859492	...	4530	2.488 ± 0.027	2.62	0.11	1.43	8.88	7.78	6.43	4.99
KIC5866965	...	4034	1.337 ± 0.029	1.41	-0.67	1.48	8.54	7.53	5.94	4.54
KIC5880651	...	4185	...	2.09	0.07	1.50	8.81	7.75	6.42	5.04
KIC5900096	...	4476	2.439 ± 0.030	2.70	0.16	1.53	8.93	7.81	6.46	5.11
KIC6125893	...	4209	1.789 ± 0.026	2.09	0.04	1.57	8.88	7.76	6.32	5.00
KIC6465075	...	4838	2.870 ± 0.031	2.82	-0.36	1.19	...	7.36	6.16	4.61
KIC6515613	...	4248	...	1.75	-0.48	1.56	8.63	7.43	5.98	4.63
KIC6547007	...	4702	2.504 ± 0.032	2.49	-0.81	1.27	...	7.12	5.79	4.28
KIC6606652	...	4230	...	1.86	-0.10	1.56	8.65	7.52	6.24	4.78
KIC6676993	...	4067	...	1.65	-0.08	1.48	8.61	7.53	6.29	4.84
KIC6680734	...	4508	2.169 ± 0.030	2.20	-0.48	1.32	8.49	7.33	5.99	4.50
KIC6696436	...	4522	2.331 ± 0.028	2.28	-0.46	1.28	8.52	7.38	6.01	4.55
KIC6784681	...	4321	...	2.17	-0.15	1.40	...	7.49	6.22	4.79
KIC6837256	...	4737	2.482 ± 0.032	2.60	-0.73	1.36	...	7.19	5.90	4.51
KIC7006979	...	4840	2.471 ± 0.034	2.66	-0.29	1.43	...	7.36	6.14	4.57
KIC7729396	...	4415	...	2.10	-0.37	1.44	8.51	7.36	6.11	4.65
KIC7889528	...	4236	...	2.10	0.03	1.57	...	7.75	6.36	4.95
KIC7950369	...	4198	...	1.98	-0.14	1.45	8.63	7.56	6.23	4.83
KIC8005874	...	4199	...	2.07	-0.13	1.40	8.63	7.57	6.24	4.84
KIC8167380	...	4266	...	1.92	-0.22	1.58	8.65	7.41	6.12	4.69
KIC8172497	...	4346	...	1.87	-0.52	1.59	8.59	7.45	5.98	4.62
KIC8617950	...	4232	...	1.94	-0.09	1.50	8.66	7.59	6.25	4.82
KIC8873797	...	4430	2.409 ± 0.027	2.37	0.01	1.43	8.81	7.86	6.41	4.97
KIC9205436	...	4206	...	1.71	-0.47	1.59	8.66	7.55	6.02	4.70

Table 6. Continued.

HIP/KIC/TYC	$T_{\text{eff,ref}}$	T_{eff}	$\log g_{\text{ref}}$	$\log g$	[Fe/H]	v_{mic}	A(O)	A(Mg)	A(Ca)	A(Ti)
KIC9326304	...	3987	...	1.29	-0.47	1.49	8.38	7.38	5.99	4.56
KIC9474021	...	3934	1.201 ± 0.030	1.34	-0.54	1.43	8.49	7.42	5.97	4.64
KIC9529652	...	3959	...	1.32	-0.55	1.47	8.46	7.42	5.95	4.63
KIC9665729	...	4048	...	1.54	-0.07	1.67	...	7.62	6.29	4.80
KIC9835672	...	3976	...	1.49	-0.19	1.52	...	7.54	6.16	4.74
KIC9969701	...	4125	...	1.74	-0.13	1.50	8.69	7.52	6.22	4.80
KIC10186608	...	4635	2.430 ± 0.030	2.56	-0.10	1.40	8.72	7.65	6.25	4.77
KIC10190244	...	4136	...	1.38	-0.94	1.62	...	7.08	5.70	4.30
KIC10403036	...	4380	1.919 ± 0.030	2.09	-0.64	1.35	8.64	7.40	5.99	4.60
KIC10649021	...	3918	1.186 ± 0.033	1.56	-0.35	1.54	8.61	7.48	5.94	4.72
KIC10802990	...	4091	...	1.49	-0.31	1.58	8.54	7.40	6.10	4.67
KIC11045542	...	4384	1.749 ± 0.028	1.84	-0.57	1.44	8.38	7.21	5.89	4.41
KIC11246393	...	4172	...	1.83	-0.22	1.43	8.58	7.46	6.19	4.76
KIC11342694	...	4429	2.815 ± 0.028	2.70	0.11	1.19	8.82	7.82	6.43	4.99
KIC11444313	...	4707	2.469 ± 0.034	2.64	-0.07	1.39	8.76	7.53	6.30	4.84
KIC11555150	...	4245	...	1.86	-0.16	1.58	...	7.51	6.20	4.77
KIC11569659	...	4813	2.424 ± 0.028	2.56	-0.38	1.42	8.51	7.37	6.11	4.51
KIC11657684	...	4816	2.437 ± 0.027	2.40	-0.41	1.48	8.56	7.22	6.08	4.50
KIC12457780	...	4174	...	1.89	-0.12	1.45	8.65	7.51	6.24	4.79
TYC324-266-1	...	4285	...	1.61	-0.89	1.49	8.39	7.15	5.85	4.39
TYC336-147-1	...	4586	...	2.47	-0.40	1.32	8.54	7.48	6.09	4.64
TYC1570-1460-1	...	4735	...	2.63	-0.41	1.51	8.82	7.63	6.13	4.79
TYC2012-1102-1	...	4193	...	1.89	-0.43	1.38	8.62	7.51	6.06	4.74
TYC2041-1586-1	...	4559	...	2.42	-0.61	1.28	...	7.41	6.00	4.62
TYC2046-759-1	...	4093	...	1.01	-1.11	1.75	8.17	6.87	5.59	4.18
TYC3026-782-1	...	4869	...	2.67	-0.70	1.34	8.66	7.33	5.96	4.53
TYC3041-648-1	...	4214	...	1.88	-0.28	1.51	8.77	7.68	6.18	4.85
TYC3044-14-1	...	4489	...	2.36	-0.15	1.49	8.77	7.71	6.25	4.85
TYC3051-805-1	...	4559	...	2.62	-0.32	1.23	8.67	7.61	6.18	4.72
TYC3051-1340-1	...	4425	...	2.08	-0.77	1.40	...	7.28	5.88	4.50
TYC3054-1026-1	...	4605	...	2.58	-0.58	1.23	8.54	7.41	6.06	4.66
TYC3058-519-1	...	4450	...	1.86	-0.76	1.68	8.55	7.36	5.79	4.46
TYC3059-694-1	...	4440	...	2.40	-0.12	1.35	8.60	7.53	6.26	4.84
TYC3064-391-1	...	4240	...	1.81	-0.73	1.40	...	7.42	5.93	4.57
TYC3064-897-1	...	4658	...	2.56	-0.28	1.44	8.74	7.63	6.17	4.82
TYC3071-1491-1	...	4725	...	2.49	-0.45	1.47	8.68	7.50	6.12	4.70
TYC3074-1109-1	...	4735	...	2.51	-0.39	1.46	...	7.50	6.10	4.68
TYC3094-1605-1	...	4309	...	1.66	-1.15	1.56	...	6.94	5.53	4.05
TYC3132-453-1	...	4436	...	1.44	-0.91	1.72	8.31	6.95	5.55	4.16
TYC3465-458-1	...	4554	...	2.54	-0.35	1.24	...	7.59	6.23	4.82
TYC3494-279-1	...	4392	...	1.73	-0.83	1.68	...	7.19	5.74	4.37
TYC3494-461-1	...	4613	...	2.41	-0.34	1.49	8.70	7.66	6.18	4.78
TYC3495-780-1	...	4880	...	2.59	-0.60	1.61	...	7.41	6.00	4.58
TYC3500-405-1	...	4679	...	2.55	-0.34	1.44	8.70	7.63	6.17	4.83
TYC3504-1938-1	...	4546	...	2.63	-0.27	1.20	8.59	7.56	6.22	4.78
TYC3844-739-1	...	4539	...	2.49	-0.08	1.48	8.83	7.76	6.33	4.93
TYC3859-503-1	...	4618	...	2.59	-0.55	1.17	...	7.53	6.12	4.69
TYC3870-557-1	...	4774	...	2.54	-0.46	1.53	8.70	7.49	6.03	4.66